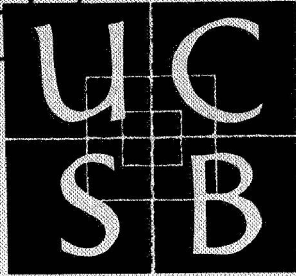
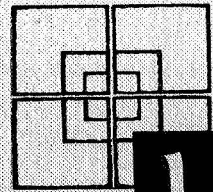


NASA CR 66821



university of california • santa barbara

THE SUPERSONIC FLIGHT OF A BLUNT BODY
IN A DISTURBED ATMOSPHERE

Jose Chirivella

**CASE FILE
COPY**

NASA GRANT NO. NGR 05-010-028

JUNE 1969

College of Engineering

NASA GRANT NO. NGR 05-010-028
JUNE 1969

SPONSORED BY
NASA LANGLEY RESEARCH CENTER
HAMPTON, VIRGINIA

THE SUPERSONIC FLIGHT OF A BLUNT BODY
IN A DISTURBED ATMOSPHERE

Jose Chirivella

Submitted in partial satisfaction of the requirements
for the degree of Doctor of Philosophy in Engineering
Science

June 1969

University of California
Department of Mechanical Engineering
Santa Barbara, California

ABSTRACT

The Supersonic Flight of a Blunt Body in a Disturbed Atmosphere

by

Jose Evangelio Chirivella

The method of integral relations has been applied to determine the field properties in the subsonic and transonic regions of the flow about a blunt axi-symmetric body. The conditions in the free stream are assumed to have sharp gradients of the Mach number and/or stagnation temperature in the direction perpendicular to the free flow. The stagnation pressure is kept constant. Four cases were run: Case I where the case for uniform free stream is solved and compared with available solutions encountered in the literature; Case II where the Mach number varies in the radial direction; Case III where the Mach number remains constant but the stagnation temperature is allowed to vary across the oncoming flow. Finally, Case IV corresponds to a simultaneous variation of the Mach number and the stagnation temperature. It is found that the most sensitive parameter to the non-uniformities is the sonic point on the body, and a general discussion and examination of the other flow parameters is carried out.

TABLE OF CONTENTS

1.	INTRODUCTION	1
2.	PHYSICAL DESCRIPTION OF THE PROBLEM	9
	2.1 Nature of Supersonic Flight under Non-Uniform Conditions	9
	2.2 The Blunt Body Problem	9
	2.3 General Approach and Numerical Techniques	11
3.	EQUATIONS OF MOTION	16
	3.1 Definition of Coordinate System	16
	3.2 Continuity Equation	16
	3.3 Momentum Equation	19
	3.4 Bernoulli Integral Equation	21
	3.5 The Entropy Equation	22
	3.6 Boundary Conditions	22
	3.7 Non-dimensionalization of the Equations of Motion	25
4.	THE METHOD OF INTEGRAL RELATIONS AND THE BLUNT BODY PROBLEM	30
	4.1 Introduction	30
	4.2 Description of the Method	31
	4.3 Accuracy, Practicability and Convergence	37
5.	APPLICATION OF THE METHOD OF INTEGRAL RELATIONS TO THE CASE OF A BLUNT BODY IN A NON-UNIFORM FLOW	42
	5.1 Introduction	42
	5.2 Formulation	42
	5.3 Study of the Fixed Singularity	52
	5.4 Moving Singularity	55

Table of Contents (continued)

5.5 Shock Layer Properties	56
5.6 Summary of Formulae	57
5.7 Numerical Procedure	63
5.8 Calculations in the Shock Layer	66
6. RESULTS	67
6.1 Description of the Different Cases under Investigation	67
6.2 Results	67
7. DISCUSSION OF RESULTS	87
8. RECOMMENDATIONS AND CONCLUSIONS	91
REFERENCES	93

LIST OF FIGURES

Fig. 1.1	EXAMPLE OF SHOCK IMPINGEMENT HEATING	4
Fig. 1.2	A FLOW PATTERN FOR THE CASE OF SHOCK IMPINGEMENT	5
Fig. 2.1	SCHEMATIC OF NON-UNIFORM BLUNT BODY PROBLEM	10
Fig. 2.2	SUPERSONIC FLIGHT OF A BLUNT BODY	12
Fig. 2.3	DIFFERENT TYPES OF SHOCK LAYERS IN THE BLUNT BODY PROBLEM	13
Fig. 2.4	SONIC LINE AND LIMITING CHARACTERISTIC	14
Fig. 3.1	COORDINATE SYSTEM	17
Fig. 3.2	ELEMENT OF VOLUME	18
Fig. 3.3	DIFFERENTIAL GEOMETRICAL RELATIONS FOR THE SHOCK	24
Fig. 4.1	CONSTRUCTION OF THE STRIPS IN THE DOMAIN OF INTEGRATION	32
Fig. 5.1	INTEGRAL CURVES FOR v_b AND SADDLE POINT	65
Fig. 6.1	DEFINITION OF INPUT PARAMETERS	68
Fig. 6.2	FLOW PATTERN FOR THE UNIFORM FLIGHT OF A SPHERE	71
Fig. 6.3	SHOCK SHAPE SOLUTION FOR CASE I BY THE ACTUAL METHOD AND BELOTSEKOVSKII'S	72
Fig. 6.4	DISTRIBUTION OF PRESSURE VERSUS n FOR VARIOUS θ	73
Fig. 6.5	FLOW PATTERN FOR CASES I AND II	74
Fig. 6.6	DISTRIBUTION OF PRESSURE ALONG n FOR VARIOUS θ FOR CASES I AND II	75
Fig. 6.7	PRESSURE DISTRIBUTION ON THE BODY FOR CASE I	76

List of Figures (continued)

Fig. 6.8	PRESSURE DIFFERENCES BETWEEN CASES II, III, IV, AND I	77
Fig. 6.9	TEMPERATURE DISTRIBUTION ALONG THE BODY	79
Fig. 6.10	STATIC TEMPERATURE DIFFERENCE FOR THE DIFFERENT CASES	80
Fig. 6.11	SHOCK WAVE SHAPES FOR THE DIFFERENT CASES	81
Fig. 6.12	VELOCITY DISTRIBUTION ON THE BODY FOR CASE I	82
Fig. 6.13	VELOCITY DISTRIBUTION ON THE BODY FOR CASE II	83
Fig. 6.14	VELOCITY DISTRIBUTION ON THE BODY FOR CASE III	84
Fig. 6.15	VELOCITY DISTRIBUTION ON THE BODY FOR CASE IV	85
Fig. 6.16	VELOCITY DISTRIBUTION DIFFERENCES FOR CASES II, III, IV, AND I	86

LIST OF TABLES

Table I	INPUT PARAMETERS	69
Table II	NUMERICAL RESULTS	69

NOMENCLATURE

Latin Characters

A	Defined by Equation (3.8). Also in paragraph 5.7, refers to the area of the cross section of a Laval nozzle
B_1	Defined by Equation (5.66)
C_1	Defined by Equation (5.65)
E_o	Defined by Equation (5.38)
F_o	Defined by Equation (5.39)
H	Defined by Equation (3.16)
L	Defined by Equation (3.9)
M	Mach number
M_c	Mach number in the free stream at two radii from the axis
M_c	Mach number in the free stream at the center line
R	Radius of curvature of the body at a generic point
S	Entropy
T	Defined by Equation (3.7)
U_1	Defined by Equation (5.47)
U_2	Defined by Equation (5.49)
V_1	Defined by Equation (5.48)
V_2	Defined by Equation (5.50)
Y	Defined by Equation (3.17)
Z	Defined by Equation (3.15)

a	Speed of sound
f	Non-dimensional distribution of q_{max}
h	Enthalpy
m	Defined in Equation (3.38)
n	Coordinate across the shock layer
p	Static pressure
q	Velocity
q_{max}	Maximum velocity attainable in a point of the free stream, by means of an isentropic expansion
q_t	Velocity component along the tangent to the shock
q_n	Velocity component along the normal to the shock
s	Coordinate along the body
u	Velocity component along n
v	Velocity component along s
x	Coordinate along the axis of symmetry
y	Radial coordinate

Greek Characters

α	Angle of the tangent to the body and the free stream
β	Angle of the tangent to the shock and the free stream.
β_c	Defined also in Section 6 as the fractional change of q_{max}
γ	Gas specific heat ratio
θ	Defined as $(\pi/2) - \alpha$
θ_{sh}^*	Azimuth of the sonic point on the shock
ξ	Non-dimensional coordinate across the shock layer defined by Equation (3.66)
ϵ	Shock stand-off distance

ρ	Density
σ	Defined as $(\pi/2) - \beta$
φ	Defined as p / ρ^γ
χ	In Section 3 represents the azimuth for that particular kind of coordinates
ψ	Stream function defined by Equation (3.56)
ω	Defined by Equation (3.33)

Subindices

at	Atmospheric conditions
b	Designates the values on the body
i	Designates values on the axis
iex	Used as ϵ_{iex} designates the exact value of ϵ_i
s	Designates values on the shock
l	Designates values on the shock in Section 5
o	Designates values on the body in Section 5. Also, in Section 3 is used to refer to values at the center line
∞	Designates values in the free stream
ls	Designates the value on the shock in a point closer to the axis than that labeled by l

Superscripts

*	Used to indicate sonic conditions
'	The primed quantities in Section 5 indicate derivatives with respect to s

1. INTRODUCTION

The supersonic flight of a blunt body has been extensively studied theoretically as well as experimentally, and there has been, during the past 15 years, a large profusion of very excellent works on the subject. A good collection of classical and recent papers on the hypersonic problems, in general, can be found in Hayes and Probstein [1.1]. Although there have been several successful solutions for special flow circumstances, the general problem remains unsolved; one can say that, in general, a particular analysis for each case is required.

A number of methods for calculating the flow of a gas past a blunt body have been developed and can be divided into two general types, direct and inverse. In the inverse method the shock shape is initially assumed known and the flow variables are expanded in a series and integrated from the shock to points in the flow field corresponding to the body streamline. Examples of these methods are given by Lomax and Inouye [1.2], Swigart [1.3], Vaglio-Laurin [1.4], and Hall et al [1.5]. Although the inverse solution is numerically exact, the problems of convergence of the series and of the extreme sensitivity of the resulting body shape have limited the application of the method. The sources of the convergence problems have been identified and usually can be avoided for smooth bodies (see Reference [1.6]).

In the direct method, the body shape is specified and the shock shape and shock layer properties are calculated. A number of direct methods have been proposed in the literature, such as the stream-tube continuity methods (see Reference [1.7]) and relaxation techniques

(see Reference [1.8]). One such method, which was developed by Gravalos, Edelfelt and Emmons [1.8], divides the flow field into three regions: a transonic region, a purely subsonic region and a purely supersonic region. Conditions in the transonic region are determined by iteration between the body and the transonic part of the shock wave. Data from this solution are used to provide boundary conditions for a solution in the subsonic region, where the equation for the stream function is solved by a relaxation technique. The solution in the supersonic region is found by the method of the characteristics. The calculations in the three regions are continued until boundary conditions at the body surface and the shock wave are all satisfied.

Another powerful direct method is based on the method of finite differences. The unsteady flow past the prescribed body shape is determined and the steady solution is found as the asymptotic form of this at large times. This approach was originally formulated by Godunov et al [1.9] and has been developed further by Bohachevsky et al [1.10] and [1.11], Moretti [1.12], and Mason [1.13].

Most of the efforts in the blunt body theory have been directed to the investigation of the aerodynamic parameters associated with the drag and heat transfer characteristics of the body submerged in a uniform flow. However, there have arisen lately some problems in which the behaviour of a body in a non-uniform supersonic stream is required. A few examples of flow situations in which the non-uniformities of the free stream have important effects on the aerodynamic behaviour of the body are as follows: a) The experimental investigation of the blunt body problem often requires the use of supersonic wind tunnels.

The flow in such tunnels, although well calibrated, may present transverse non-uniformities due, for example, to the intentional heating of flow in the tunnel; this heating is sometimes necessary, for example, to avoid the formation of condensation waves which tend to form at relatively large Mach numbers if the stagnation enthalpy is not increased. Other non-uniformities that could possibly be encountered in a supersonic wind tunnel are those that contribute to losses of stagnation pressure along and across the stream, i.e., weak shocks and boundary layer effects. b) In the supersonic flight of certain aircraft an anomalous phenomenon has been observed. This phenomenon is produced by the impingement of a shock on the bow shock of another body, illustrated in Figure 1.1. Here the bow shock of the fuselage interferes with the bow shock of the booster. This impingement is extraordinarily difficult to analyze and depending on the initial and boundary conditions the flow pattern in the interference region may be totally different as has been proved experimentally by Edney [1.14]. All of the different configurations have one thing in common and this is a significant rise in the heat transfer rate to the wall of the body in the vicinity of the impingement. It seems that the highest heat rate corresponds to the case where a non-uniform supersonic stream formed behind the shock intersection impinges on the wall of the body. There has not been so far a theoretical effort to investigate the origin of this striking increase in the heat transfer rate. A schematic picture of the situation can be seen in Figure 1.2. c) Another case of possible interest would be the impingement of the exhaust plume of a rocket on a body whose size is of the order of magnitude of the diameter of

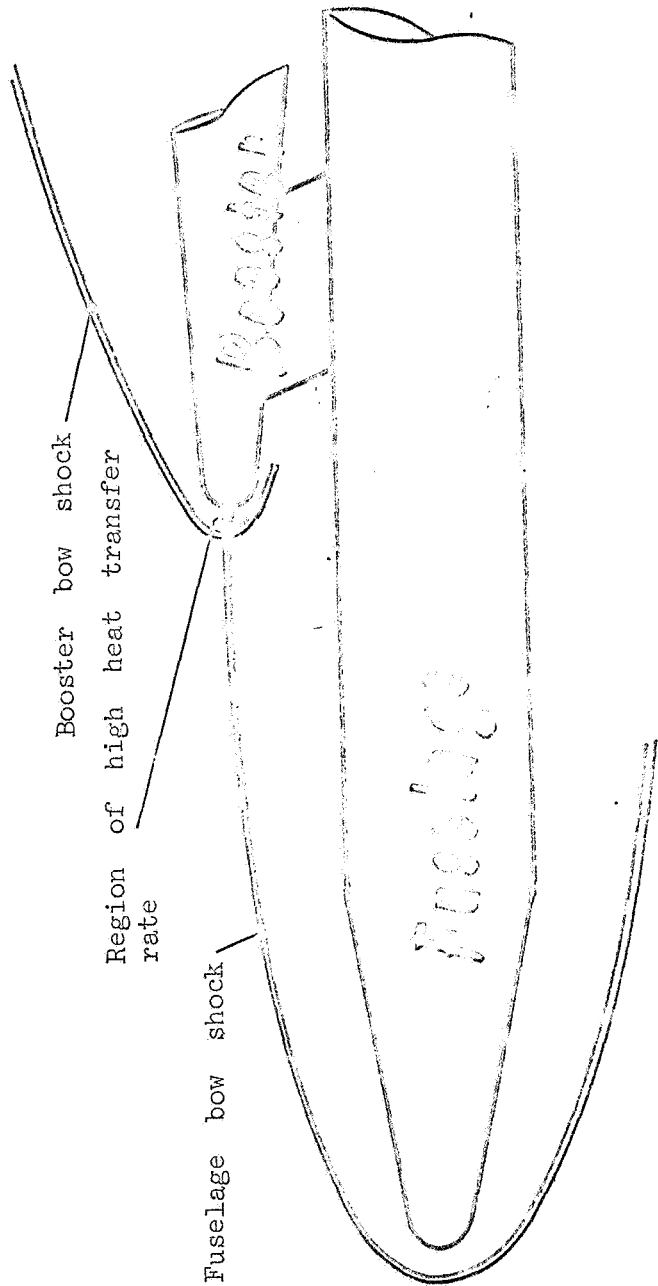


FIG. 1.1.1 EXAMPLE OF SHOCK IMPINGEMENT HEATING

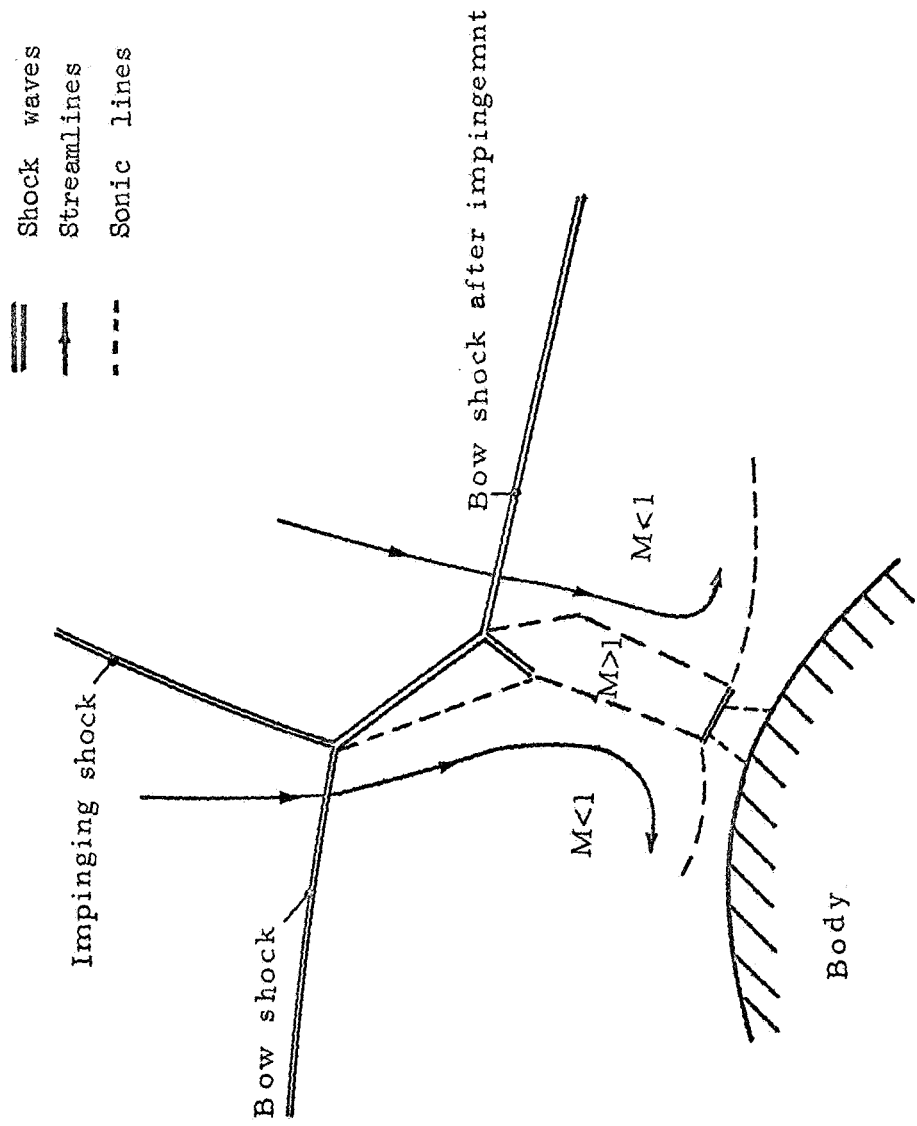


FIG. 1.2 A FLOW PATTERN FOR THE CASE OF SHOCK IMPINGEMENT

the plume. This situation occurs, for example, in the separation of rocket stages.

The above considerations have led to an investigation of the effects of the non-uniformities of the free stream on the flow field properties in the shock layer and their importance as compared with the case of having uniform flow in the free stream. As a first effort to analyze such effects, the following physical model is considered:

- a) The oncoming stream will always be supersonic.
- b) The flow will be inviscid, i.e., viscosity effects are neglected.
- c) The streamlines upstream of the shock will be parallel.
- d) The body to be investigated will have axial symmetry and its angle of attack zero.
- e) The stagnation pressure in the free stream will remain constant.
- f) The Mach number and/or the stagnation temperature of the free flow will vary perpendicular to the flow direction. These distributions of non-uniformities will also be assumed to have axial symmetry.
- g) The gas will be assumed to be calorically and thermally perfect.

Although the model does not represent physically all the different situations mentioned above, it seems to be, on the other hand, an excellent representation of the supersonic wind tunnel case. Nevertheless, it will throw some light on the understanding of the more complicated

cases such as the shock impingement case or the plume impact on the separated rocket stage.

In this dissertation, the inviscid flow field in the mixed flow regions is determined by the method of integral relations developed for the case of uniform free stream by Belotserkovskii [1.15] (for a complete literature survey on the method and a general discussion, see Section 4). In this case certain quantities are interpolated as linear functions between the body and the shock; the equations of motion are then written in divergence form, integrated across the shock layer, and replaced by a set of ordinary differential equations to determine the velocity on the body, the shock detachment distance, and the shock angle.

The method requires the integration of the approximating system of ordinary differential equations between the axis and the sonic point. On a smooth contour body this point is located at a saddle point singularity in the body velocity derivative. The shock detachment distance on the axis must be chosen so that the solution is regular at the saddle point. The procedure for determining this has been considerably simplified since the method was first applied and the converged solution, together with conditions at and beyond the sonic point, can now be found after very few iterations.

Four cases have been investigated under the present method: Case I, in which the free stream is considered uniform; Case II with a variation of Mach number in the free stream; Case III with uniform Mach number in the free stream but allowing a stagnation temperature variation; Case IV where a simultaneous variation of stagnation

temperature and Mach number are considered. Case I is compared with the more exact and elaborate Belotserkovskii's solution. The approximation seems to be excellent and only in the vicinity of the sonic line separates slightly from Belotserkovskii's solution. A discussion of the results can be found in Section 7 where Cases II, III, IV are compared with Case I.

2. PHYSICAL DESCRIPTION OF THE PROBLEM

2.1 Nature of the Supersonic Flight under Non-Uniform Conditions

The considerations discussed in Section 1 have led to an investigation of the supersonic flight of a blunt body under non-uniform conditions in the free flow defined as follows (see Figure 2.1):

Let Ω be a body of revolution with no singularities along the surface, and $O-x$ be the axis of symmetry. Consider now an oncoming supersonic flow whose streamlines are all parallel to the axis $O-x$ and whose Mach number and stagnation temperature vary along the radial coordinate y . The stagnation pressure will be assumed to be constant throughout the free flow. As a consequence of the presence of the body, a shock wave will appear at the bow of the body in a similar manner as occurs in the classical blunt body problem. The non-uniformities will be assumed to be symmetrically distributed, and an investigation of their propagation across the shock and their effects on the aerodynamic and thermal properties of the body will be the subject of this dissertation.

2.2 The Blunt Body Problem

Due to the parallelism of the actual problem with the classical blunt body problem, a review of the salient features for that case is given in the present Section.

In the flight of a blunt body at supersonic speeds, a detached shock wave travels with the body. The region between the shock and the body is called the shock layer and the flow in such a region is of a

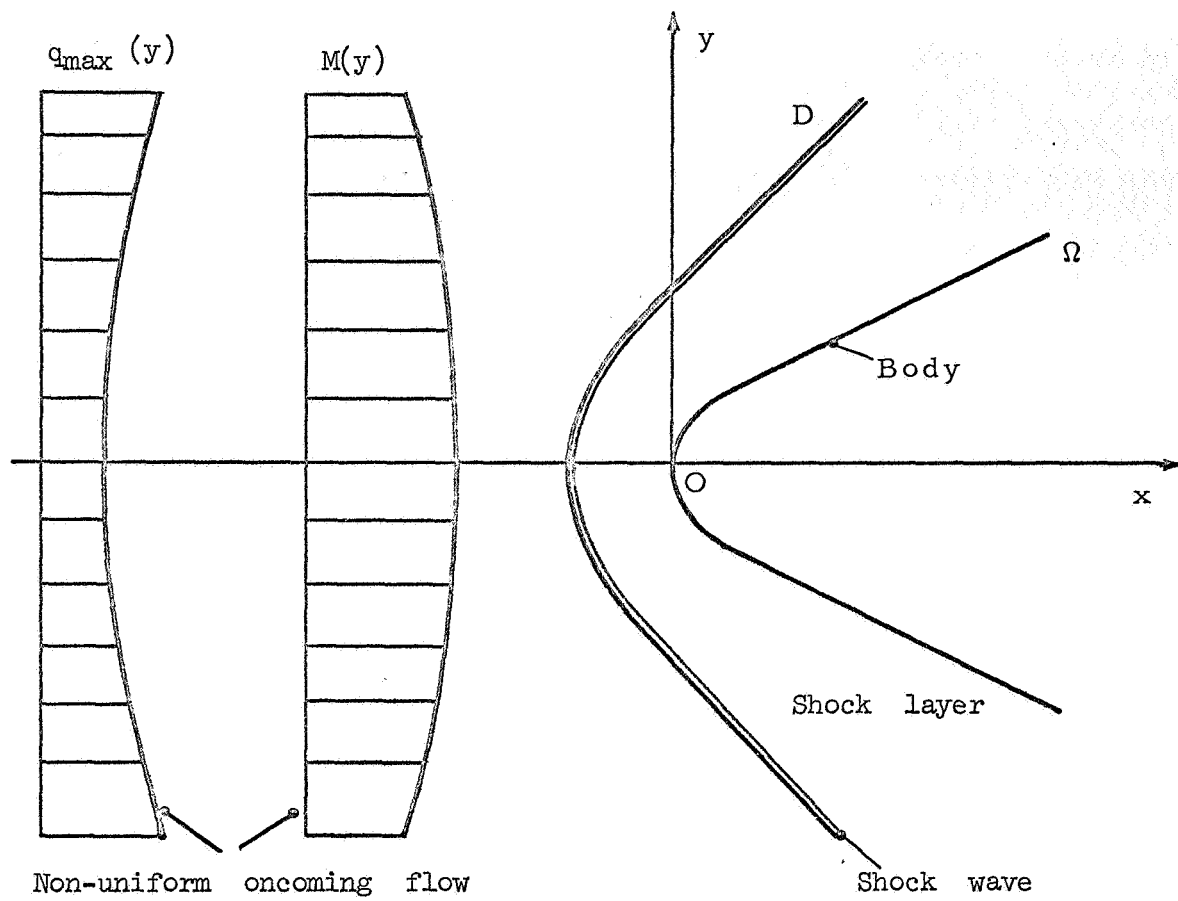


FIG. 2.1 SCHEMATIC OF NON-UNIFORM BLUNT BODY PROBLEM

transonic nature, i.e., the governing differential equations are of the hyperbolic-elliptic type (see Figure 2.2).

The line along which the Mach number is one, is designated the sonic line, and of particular importance is the relative location of the points P, Q at which the sonic line intersects the shock and the body. The shape of the sonic line, depending on the body shape and the free stream Mach number, may be one of the three types shown in Figure 2.3. One important feature of the region on the supersonic side of the sonic line and extending to the limiting characteristic defined below, is that the flow is pseudo-elliptic in the sense that even though the flow is supersonic, perturbations are propagated upstream. This results from the occurrence of the intersection of the characteristics in this region with the sonic line thus affecting the subsonic region (see Figure 2.4). Note that one defines the limiting characteristic as the locus of points for which the characteristics intersect the sonic line at one point and only one; for example, in Figure 2.4 it would be the line QP'. In Figure 2.3 the limiting characteristic for the different cases are indicated. Once the limiting characteristic and the flow field variables along it are known, the flow downstream is easily calculated by the powerful "method of the characteristics". For a general discussion of the blunt body problem see, for example, Hayes and Probstein [2.1].

2.3 General Approach and Numerical Techniques

Because of the similarity of the problem with the blunt body one, analytic and numerical techniques available for this problem have

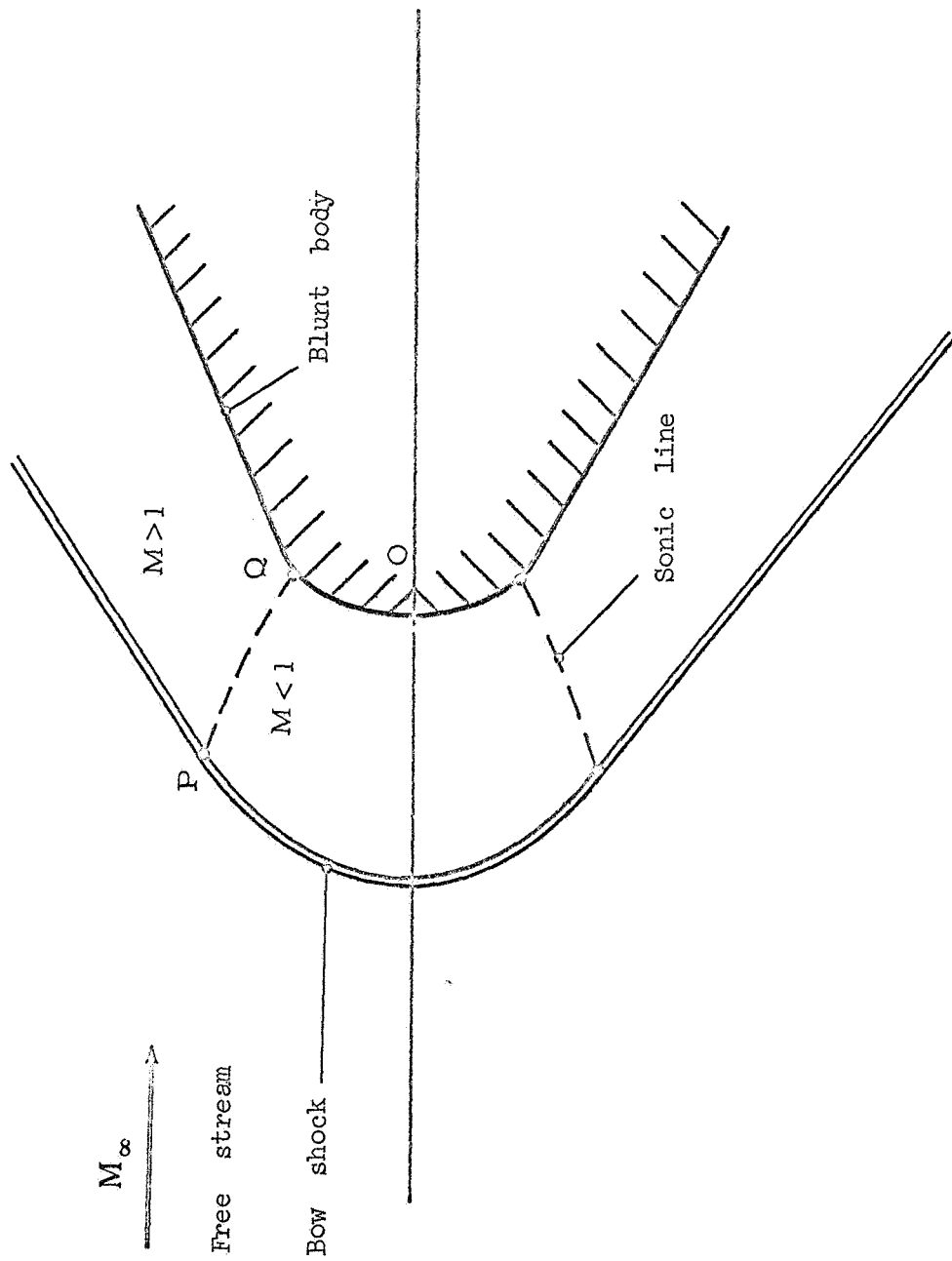
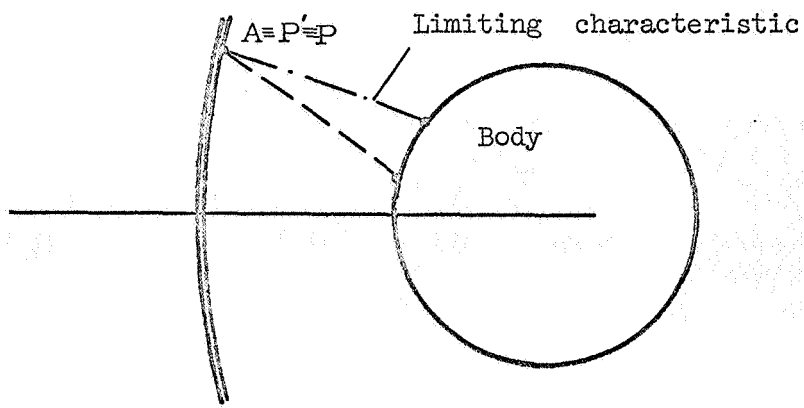
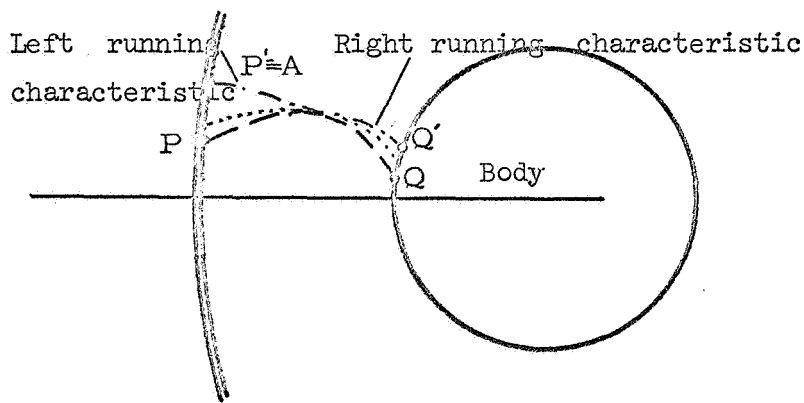


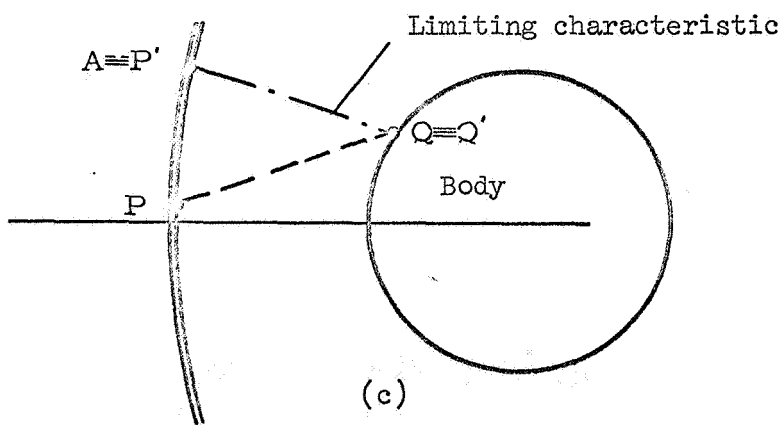
FIG. 2.2 SUPERSONIC FLIGHT OF A BLUNT BODY



(a)



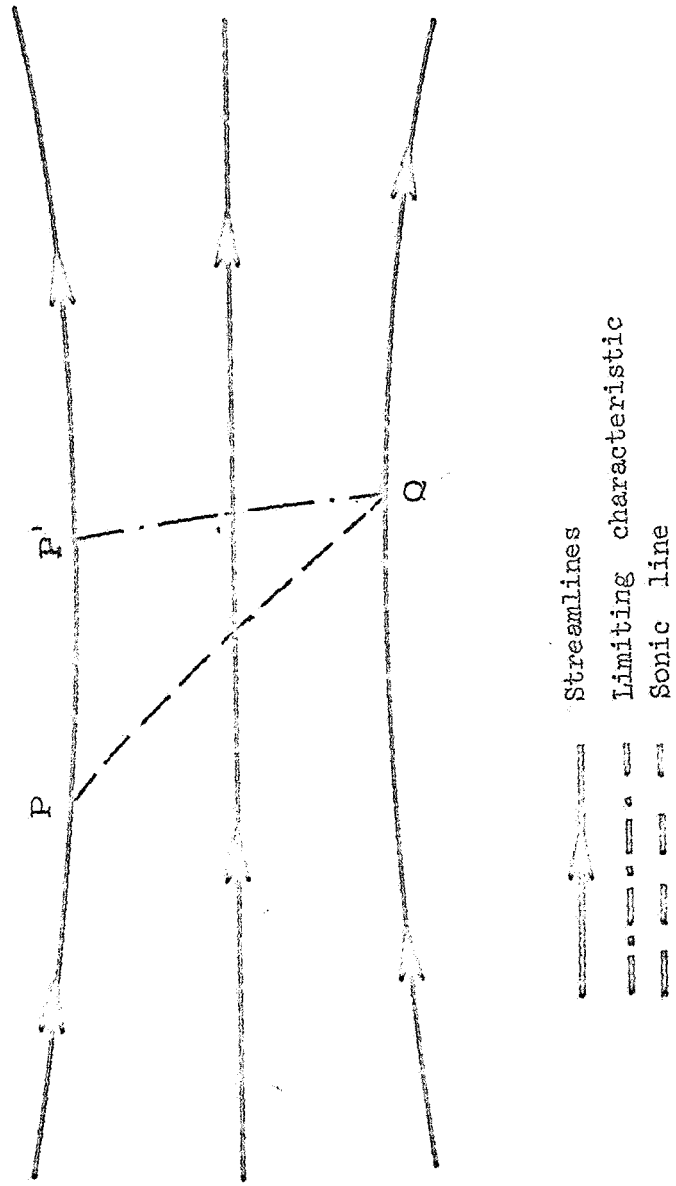
(b)



(c)

- Limiting characteristic
- - - Sonic line
- ==== Shock wave

FIG. 2.3 DIFFERENT TYPES OF SHOCK LAYERS IN THE BLUNT BODY PROBLEM




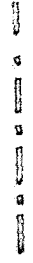
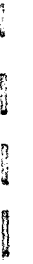
 Streamlines
 Limiting characteristic
 Sonic line

FIG. 2.4 SONIC LINE AND LIMITING CHARACTERISTIC

been reviewed for their possible application to the actual case (see also Introduction). Among the analytical techniques used in blunt body investigations (i.e., streamtube continuity method) most of them have the peculiarity that the assumption of a uniform free stream is very restrictive and their possible extension to our problem is not seen to be easy. If one restricts the free stream variations to conical-like flows, Eastman and Bonnema [2.7] and [2.8] have applied the inverse method and obtained a solution. These results however have limited application to the variations noted in the introduction. Nevertheless, these analytical techniques should still be subject to further consideration and their possible application is left open.

Among the finite difference methods most commonly used are the method of artificial viscosity, which requires very detailed mesh calculations (see for example the papers of Lax [2.2] and [2.3]), and Godunov's method [2.4], which, although only of first degree accuracy, is especially powerful in that it handles the shock as a discontinuity and thus only requires a very small number of mesh points (see References [2.4], [2.5], and [2.6]). Godunov's method seems adequate and it should be pursued further. However, attention was turned to the method of integral relations which has been shown to be one of the most accurate in many blunt body calculations. For further details on the method see Section 4 where the method is widely discussed.

3. EQUATIONS OF MOTION

3.1 Definition of Coordinate System

Let Ω be a body of revolution and let us take the axis x as the axis of symmetry of the body (Figure 3.1). Now a coordinate system $P(n,s)$ is considered, where n is the distance from the point P to the body measured along the normal, s is the distance along the body arc from the center point O to the point M where the normal through P intersects the body Ω . If the free flow has an axi-symmetric distribution of Mach number and stagnation temperature, the resulting flow will be axi-symmetric with zero component in the azimuthal direction. The differential equations of motion can be found by considering a volume element dV as described in Figure 3.2. The components of the velocity \vec{q} will be given by u and v along n and s respectively.

3.2 Continuity Equation

$$d[\rho u \text{ area}(ABCD)] + d[\rho v \text{ area}(CDC'D')] = 0 \quad (3.1)$$

but

$$\text{area}(ABCD) = y d\chi (R + n) d\theta \quad (3.2)$$

$$\text{area}(CDC'D') = y d\chi dn \quad (3.3)$$

where (see Figure 3.1) R is the radius of curvature of the body Ω at the point M , y is the distance from P to the axis of symmetry,

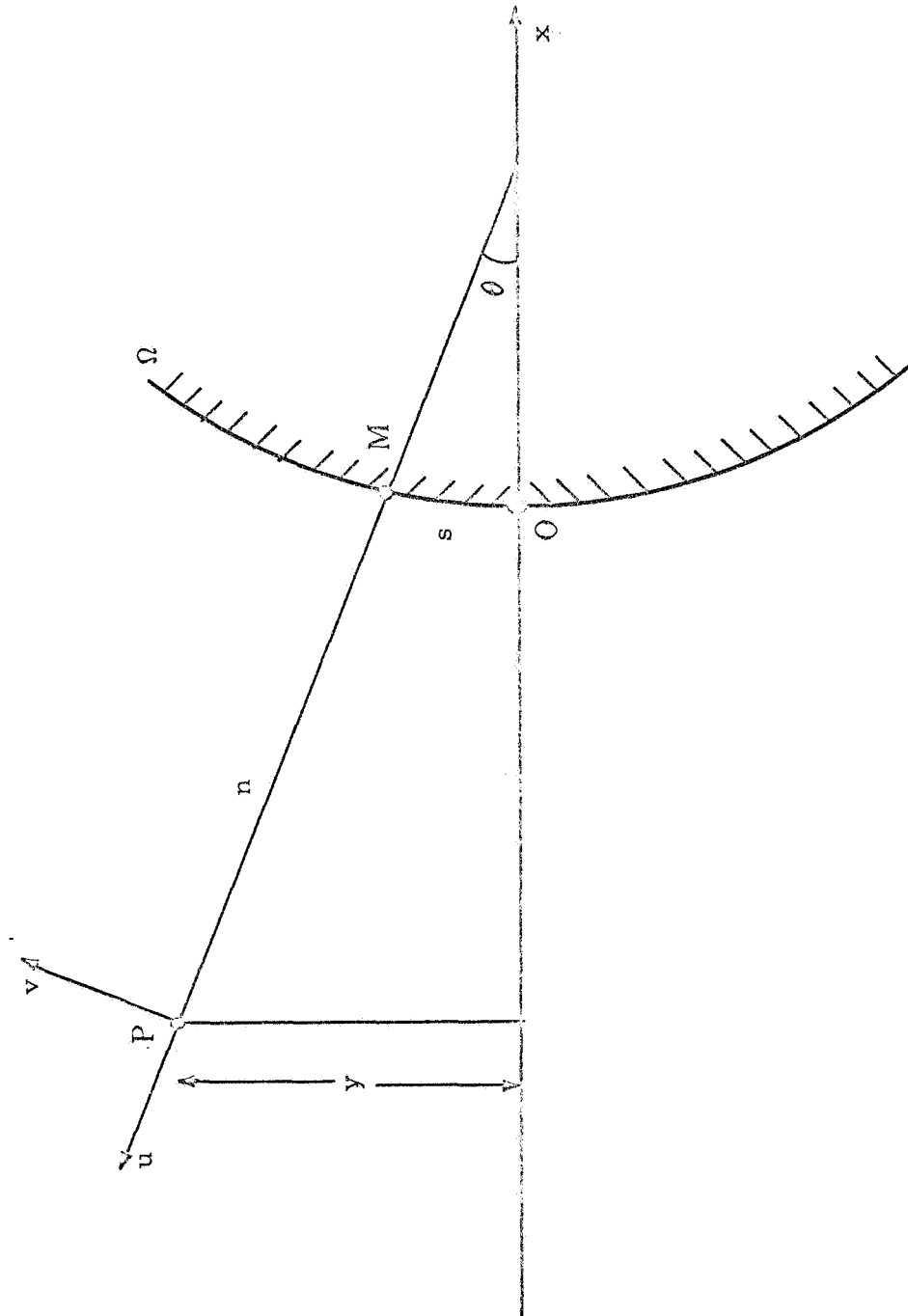
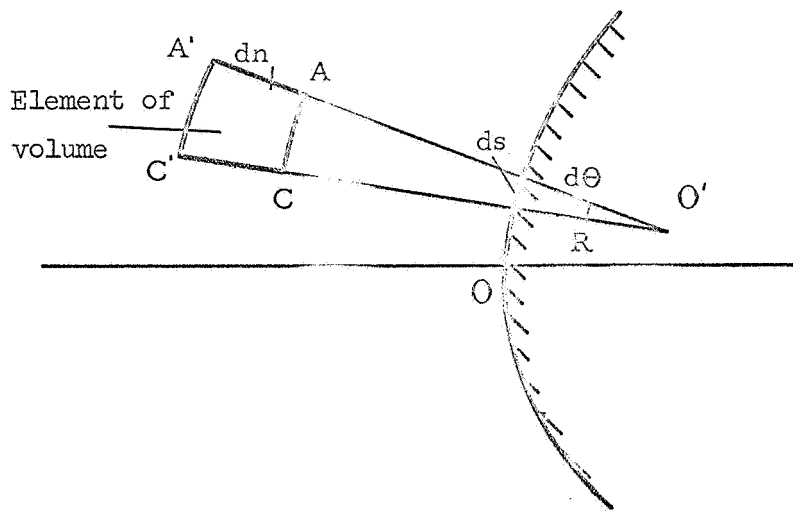
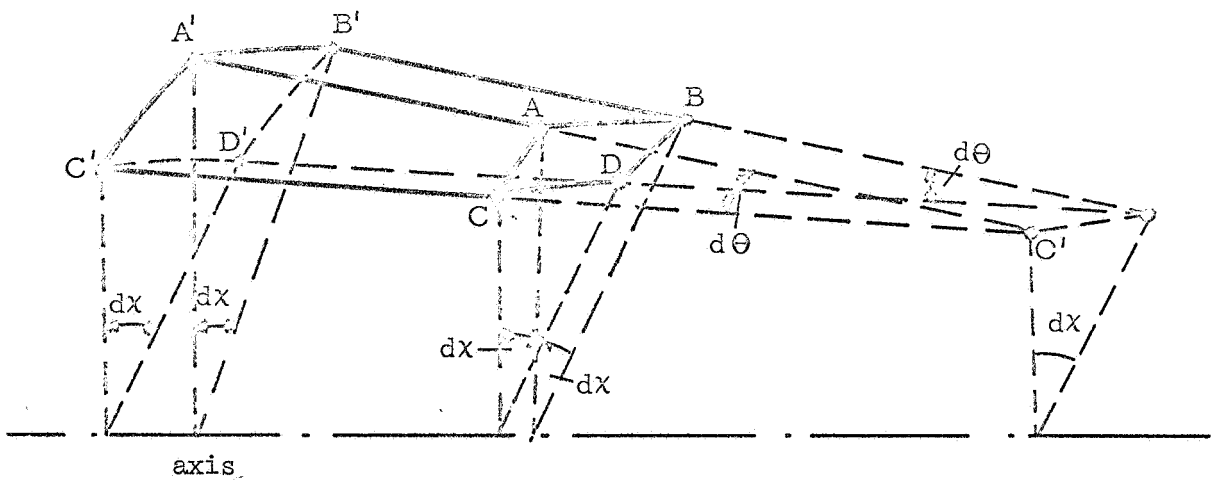


FIG. 3.1.1 COORDINATE SYSTEM



(a)

Projection of the element of volume on the meridian plane



(b)

General geometry of the element of volume

FIG. 3.2 ELEMENT OF VOLUME

θ is the angle formed by \overline{PM} and the axis $O-x$, and $d\chi$ the elemental change of azimuthal angle. Taking (3.2) into (3.1) and expanding the differentials, one gets

$$\frac{\partial}{\partial n} \left[\rho u y (R + n) \right] d\chi d\theta dn + \frac{\partial(\rho v y)}{\partial s} d\chi ds dn = 0 \quad (3.4)$$

or

$$\frac{1}{R} \frac{\partial}{\partial n} \left[\rho u y (R + n) \right] + \frac{\partial(\rho v y)}{\partial s} = 0 \quad (3.5)$$

hence the equation of continuity can be written in the form

$$\frac{\partial T}{\partial s} + \frac{\partial(A L)}{\partial n} = 0 \quad (3.6)$$

where

$$T = \rho v y \quad (3.7)$$

$$A = 1 + \frac{n}{R} \quad (3.8)$$

$$L = \rho u y \quad (3.9)$$

3.3 Momentum Equation

Here, we should have two scalar equations. One, the equation of motion in the projection on n and the other one on s . Only one of these equations will be needed if the Bernoulli equation and the con-

servation of the entropy are brought in, and therefore only the equation along n will be considered here. Thus

$$\begin{aligned} d[\rho u^2 \text{area}(ABCD)] + d[\rho u v \text{area}(CDC'D')] = \\ \rho v^2 \text{area}(CDC'D') d\theta - d[p \text{area}(ABCD)] + \\ p \text{area}(CDC'D') d\theta + p \text{area}(AA'CC') dx \sin \theta \end{aligned} \quad (3.10)$$

and expanding the differentials and taking into account (3.2) and

$$\text{area}(AA'CC') = (R + n) dn d\theta \quad (3.11)$$

one gets then

$$\begin{aligned} \frac{\partial}{\partial n} [(\rho u^2 + p) y (R + n)] + \frac{\partial}{\partial s} (\rho u v y) R - \\ \rho v^2 y = p [y + (R + n) \sin \theta] \end{aligned} \quad (3.12)$$

or

$$\begin{aligned} \frac{\partial}{\partial s} (\rho u v y) + \frac{\partial}{\partial n} [(\rho u^2 + p) y \left(1 + \frac{n}{R}\right)] = \\ p \left(1 + \frac{n}{R}\right) \sin \theta + (\rho v^2 + p) \frac{y}{R} \end{aligned} \quad (3.13)$$

or in condensed form

$$\frac{\partial Z}{\partial s} + \frac{\partial (A H)}{\partial n} = Y \quad (3.14)$$

where

$$Z = \rho u v y \quad (3.15)$$

$$H = (p + \rho u^2) y \quad (3.16)$$

$$Y = (p + \rho v^2) \frac{y}{R} + A p \sin \theta \quad (3.17)$$

3.4 Bernoulli Integral Equation

Along a streamline

$$\frac{1}{2} q^2 + h = \frac{1}{2} q_{\max}^2 \quad (3.18)$$

where h is the enthalpy and q_{\max} is the maximum velocity that can be obtained by a total isentropic expansion. If the perfect gas approximation is brought in, equation (3.18) becomes

$$\frac{1}{2} q^2 + \frac{\gamma}{\gamma-1} \frac{p}{\rho} = \frac{1}{2} q_{\max}^2 \quad (3.19)$$

This equation is valid even across a shock wave, and if the oncoming flow is isoenergetic, i.e. q_{\max}^2 is constant, it is valid for the whole region. Let us assume for the moment that it is a function of y , i.e.

$$q_{\max} = q_{\max}(y) \quad (3.20)$$

3.5 The Entropy Equation

One of the features of inviscid flow is that if the flow is continuous, the entropy is constant along a trajectory. If the flow is steady, a streamline is a trajectory and, thus, downstream of the shock

$$S = S(\Psi) = \text{constant along a streamline} \quad (3.21)$$

where Ψ is the stream function defined by

$$\rho v y = \frac{\partial \Psi}{\partial n} \quad (3.22)$$

$$\left(1 + \frac{n}{R}\right) \rho u y = - \frac{\partial \Psi}{\partial s} \quad (3.23)$$

3.6 Boundary Conditions

On the body, where $n = 0$, one has

$$u_b(s) = 0 \quad (3.24)$$

$$\Psi_b(s) = 0 \quad (3.25)$$

$$S_b(s) = \text{constant} \quad (3.26)$$

and at the axis, where $s = 0$,

$$v_o(n) = 0 \quad (3.27)$$

$$\Psi_o(n) = 0 \quad (3.28)$$

$$S_o(n) = S_b(s) = \text{constant} \quad (3.29)$$

The boundary conditions on the shock, i.e. $n = \epsilon(s)$, are

$$\Psi_s = \int_0^y y \rho_\infty q_\infty dy \quad (3.30)$$

$$p_s = p_\infty \left[1 + \frac{2\gamma}{\gamma+1} (M_\infty^2 \cos^2 \sigma - 1) \right] \quad (3.31)$$

$$\rho_s = \rho_\infty \frac{(\gamma + 1) M_\infty^2 \cos^2 \sigma}{(\gamma - 1) M_\infty^2 \cos^2 \sigma + 2} \quad (3.32)$$

$$\omega_s = \tan^{-1} \left[2 \tan \sigma \frac{M_\infty^2 \cos^2 \sigma - 1}{M_\infty^2 (\gamma - \cos 2\sigma) + 2} \right] \quad (3.33)$$

$$M_s^2 = \frac{1 + \frac{\gamma-1}{2} M_\infty^2 \cos^2 \sigma}{\gamma M_\infty^2 \cos^2 \sigma - \frac{\gamma-1}{2}} \frac{1}{\cos^2(\sigma + \omega_s)} \quad (3.34)$$

$$q_s = M_s \left(\gamma \frac{p_s}{\rho_s} \right)^{\frac{1}{2}} \quad (3.35)$$

where ω_s is the local deflection of the flow, M_s is the Mach number behind the shock, p_∞ is for this case the atmospheric pressure p_{at} , q_s is the velocity of the flow behind the shock and σ is the angle of the shock with respect to the perpendicular to the free stream.

The angle σ is related to the stand-off distance by (see Figure 3.7)

$$d\epsilon = - (R + \epsilon) \tan(\sigma - \theta) \frac{ds}{R} \quad (3.36)$$

or

$$\frac{d\epsilon}{ds} + \left(1 + \frac{\epsilon}{R} \right) \tan(\sigma - \theta) = 0 \quad (3.37)$$

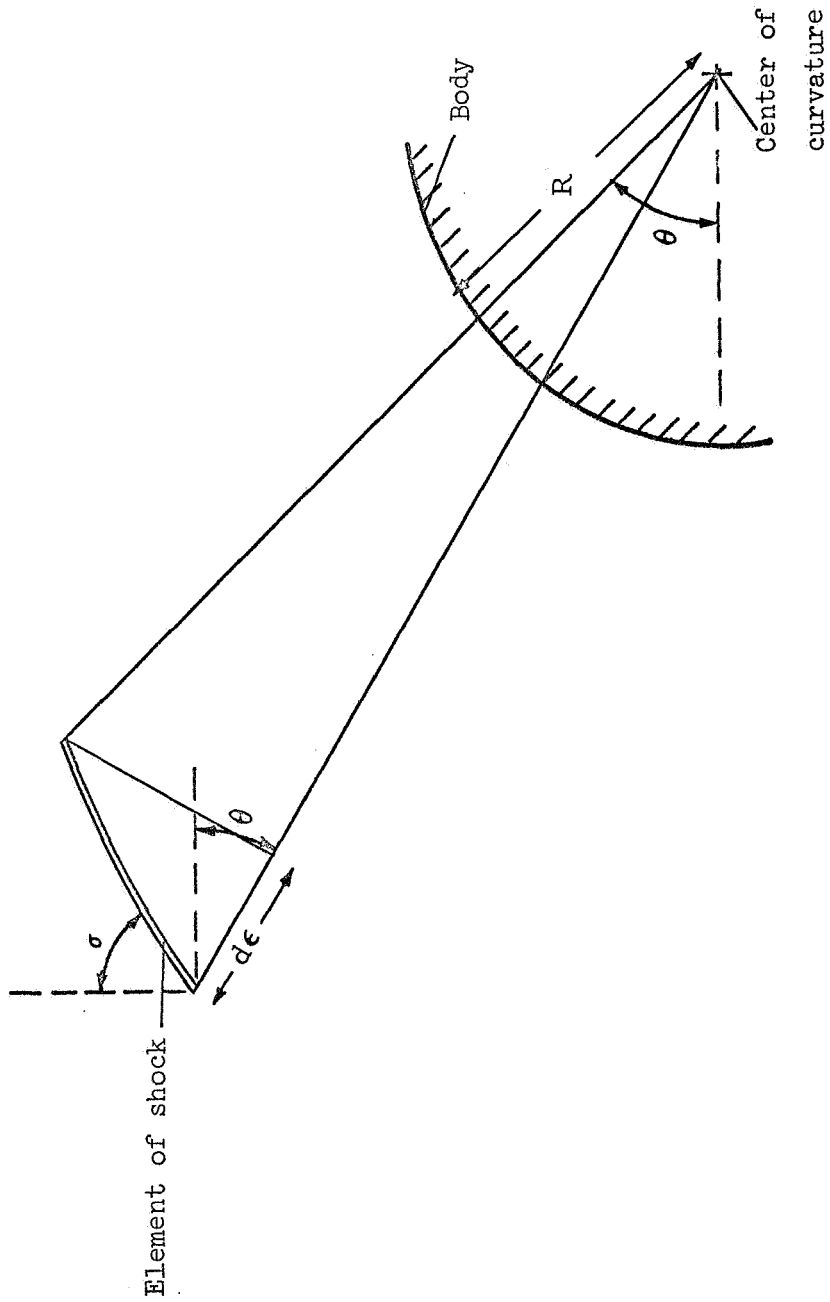


FIG. 3.3 DIFFERENTIAL GEOMETRICAL RELATIONS FOR THE SHOCK

3.7 Non-dimensionalization of the Equations of Motion

Taking into account that the stagnation pressure upstream of the shock is constant and that the Mach number throughout the free flow is greater than one, let us make

$$M_\infty = 1 + m(y) \quad (3.38)$$

with $m(y) \geq 0$.

From the Bernoulli equation (3.19) one has

$$\frac{q_\infty}{q_{\max}} = \left[\frac{\frac{\gamma-1}{2} M_\infty^2}{1 + \frac{\gamma-1}{2} M_\infty^2} \right]^{\frac{1}{2}} \quad (3.39)$$

but since q_{\max} varies with y , one has

$$q_{\max} = q_{\max 0} f(y) \quad (3.40)$$

where $f(0) = 1$. It should be remarked that the distribution of q_{\max} is the square of the distribution of the stagnation temperature.

Given $f(y)$ and $m(y)$, the density distribution is given by

$$\frac{1}{2} q_\infty^2 + \frac{\gamma}{\gamma-1} \frac{P_\infty}{\rho_\infty} = \frac{1}{2} q_{\max}^2 \quad (3.41)$$

hence

$$\rho_\infty = \frac{2 \gamma}{\gamma-1} \frac{P_\infty}{q_{\max}^2 - q_\infty^2} \quad (3.42)$$

with

$$P_\infty = P_{\infty 0} \left(1 + \frac{\gamma-1}{2} M_\infty^2 \right)^{-\frac{\gamma}{\gamma-1}} \quad (3.43)$$

Equation (3.41) for $q_{\infty} = 0$ becomes

$$\frac{\gamma}{\gamma-1} \frac{p_{\infty 0}}{\rho_{\infty 0}} = \frac{1}{2} q_{\max 0}^2 \quad (3.44)$$

After these considerations, Equation (3.41) can be rewritten as

$$\frac{1}{2} \frac{q_{\infty}^2}{q_{\max 0}^2} + \frac{\gamma}{\gamma-1} \frac{\frac{p_{\infty}}{p_{\infty 0}} \frac{2\gamma/(\gamma-1)}{\rho_{\infty}}}{\frac{\rho_{\infty}}{\rho_{\infty 0}}} = \frac{1}{2} \quad (3.45)$$

Thus, the pressure will be non-dimensionalized by the expression $p_{\infty 0} 2\gamma/(\gamma-1)$, the velocity by $q_{\max 0}^2$, the density by $\rho_{\infty 0}$, and the length by the radius of curvature R_0 of the body at the stagnation point. Subscripts o refer to the stagnation conditions.

With this non-dimensionalization, the dimensionless equations of motion are:

Continuity

$$\frac{\partial T}{\partial s} + \frac{\partial(A L)}{\partial n} = 0 \quad (3.46)$$

with

$$T = \rho v y \quad (3.47)$$

$$A = 1 + \frac{n}{R} \quad (3.48)$$

$$L = \rho u y \quad (3.49)$$

n-Momentum

$$\frac{\partial Z}{\partial s} + \frac{\partial(A H)}{\partial n} = Y \quad (3.50)$$

where

$$Z = \rho u v y \quad (3.51)$$

$$A = 1 + \frac{n}{R} \quad (3.52)$$

$$H = y (p + \rho u^2) \quad (3.53)$$

$$Y = (p + \rho v^2) \frac{y}{R} + A p \sin \theta \quad (3.54)$$

Note that although (3.46) to (3.54) appear the same as (3.7) to (3.9) and (3.14) to (3.17), it should be remarked that the variables in the present equations are dimensionless. The same symbols have been used for the present non-dimensional variables for clarity in nomenclature.

The Bernoulli equation becomes

$$p = \rho \frac{Y-1}{2Y} \left[f(y)^2 - q^2 \right] \quad (3.55)$$

The dimensionless stream function is defined by

$$d\Psi = \rho y \left[v \, dn - \left(1 + \frac{n}{R} \right) u \, ds \right] \quad (3.56)$$

If a more convenient function

$$\varphi = \frac{p}{\rho Y} \quad (3.57)$$

is defined it is evident that along a streamline

$$\varphi = \varphi(\Psi) = \text{constant} \quad (3.58)$$

can be used to replace the entropy equation.

The boundary conditions along the body, $n = 0$, are

$$u_b(s) = 0 \quad (3.59)$$

$$\Psi_b(s) = 0 \quad (3.60)$$

$$\varphi_b(\Psi_b) = \text{constant} \quad (3.61)$$

At the axis, $s = 0$, one has

$$v_o(n) = 0 \quad (3.62)$$

$$\Psi_o(n) = 0 \quad (3.63)$$

$$\varphi_o(\Psi_o) = \varphi_b(\Psi_b) = \text{constant} \quad (3.64)$$

Behind the shock one has from equation (3.37)

$$\frac{d\epsilon}{ds} + \left(1 + \frac{\epsilon}{R}\right) \tan(\sigma - \theta) = 0 \quad (3.65)$$

The Rankine-Hugoniot relations given by equations (3.30) through (3.35) remain the same after the non-dimensionalization.

The differential equations (3.46) and (3.50) can be transformed in a more convenient form if one adopts the customary boundary layer coordinates, i.e.

$$n = \xi \epsilon \quad (3.66)$$

$$s = s \quad (3.67)$$

Then

$$\left(\frac{\partial}{\partial s}\right)_n = \left(\frac{\partial}{\partial s}\right)_\xi - \frac{\xi \epsilon'}{\epsilon} \left(\frac{\partial}{\partial \xi}\right)_s \quad (3.68)$$

$$\left(\frac{\partial}{\partial n}\right)_s = \frac{1}{\epsilon} \left(\frac{\partial}{\partial \xi}\right)_s \quad (3.69)$$

where the primed quantities denote differentiation with respect to s .

The transformed equations (3.46) and (3.50) are thus

$$\frac{\partial T}{\partial s} - \xi \frac{\partial}{\partial \xi} \left(\frac{\epsilon'}{\epsilon} T \right) + \frac{\partial}{\partial \xi} \left(\frac{A L}{\epsilon} \right) = 0 \quad (3.70)$$

$$\frac{\partial Z}{\partial s} - \xi \frac{\partial}{\partial \xi} \left(\frac{\epsilon'}{\epsilon} Z \right) + \frac{\partial}{\partial \xi} \left(\frac{A H}{\epsilon} \right) = Y \quad (3.71)$$

Since ξ is the distance from the body to the shock measured along the normal, then $\xi = 0$ on the body and $\xi = 1$ on the shock.

4. THE METHOD OF INTEGRAL RELATIONS AND THE BLUNT BODY PROBLEM

4.1 Introduction

The strip method of integral relations is due to Dorodnitsyn, who extended the N-parameter formulation of Galerkin and Kantarovich to the present form of the method. A very good survey of earlier developments and applications can be found in Bethel [4.1]. An abstract describing the general method appears in Dorodnitsyn [4.2]. In reference [4.3], Belotserkovskii and Chushkin allude to a more detailed report of the work. Subsequently, Dorodnitsyn [4.4] published an exposition of the method, and still later, generalized the method (references [4.5] and [4.6]) in an effort to increase the accuracy without a corresponding increase in machine time.

The best elaboration of the method for the blunt body problem is due to Belotserkovskii, who has carried out computations for a large number of cases, obtaining an astonishing accuracy for relatively short machine times (see for example Belotserkovskii [4.7] and [4.8]). For more recent publications with an extension of the method to the case of non-equilibrium chemistry, see Belotserkovskii et. al. [4.9] and [4.10]. A variation of the method for the case of non-equilibrium flows can be found in Gilinskii et. al. [4.11]. In the U.S.A. the method has not been widely used yet, but the reader is referred among others to Gold and Holt [4.12], Deacon and Oliver [4.13], Kuby et. al. [4.14] and Holt who has applied the method to many blunt body and boundary layer problems (a partial list of Holt's works appears as a reference in Belotserkovskii's and Chushkin's article on the method [4.15]).

4.2 Description of the Method

Although there have been some applications in three dimensions [4.16], we will restrict ourselves to the case where the physical model can be well described by two coordinates, i.e. two-dimensional and axis-symmetric problems. Let us assume that the governing differential equations of the problem are

$$\frac{\partial}{\partial x} P_{\ell}(x,y,u_1,u_2,\dots,u_L) + \frac{\partial}{\partial y} Q_{\ell}(x,y,u_1,u_2,\dots,u_L) = F_{\ell}(x,y,u_1,u_2,\dots,u_L) \quad , \quad (\ell = 1,2,\dots,L) \quad (4.1)$$

where x and y are the independent variables, u_1, u_2, \dots, u_L are the unknowns, P, Q, F are known functions of $x, y, u_1, u_2, \dots, u_L$. Let the solution of the system be required in a region of the shape of a curvilinear quadrangle with boundaries (see Figure 4.1) :

$$x = a \quad , \quad x = b \quad , \quad y = 0 \quad , \quad y = \Delta(x)$$

Concerning the boundary conditions of the system (4.1) we shall assume them to be

$$\left. \begin{array}{l} \text{at } x = a \\ \varphi_{\nu}(y, u_1, u_2, \dots, u_L) = 0 \\ \nu = 1, 2, \dots, h \\ \\ \text{at } x = b \\ \varphi_{\nu}(y, u_1, u_2, \dots, u_L) = 0 \\ \nu = h+1, h+2, \dots, L \end{array} \right\} \quad (4.2)$$

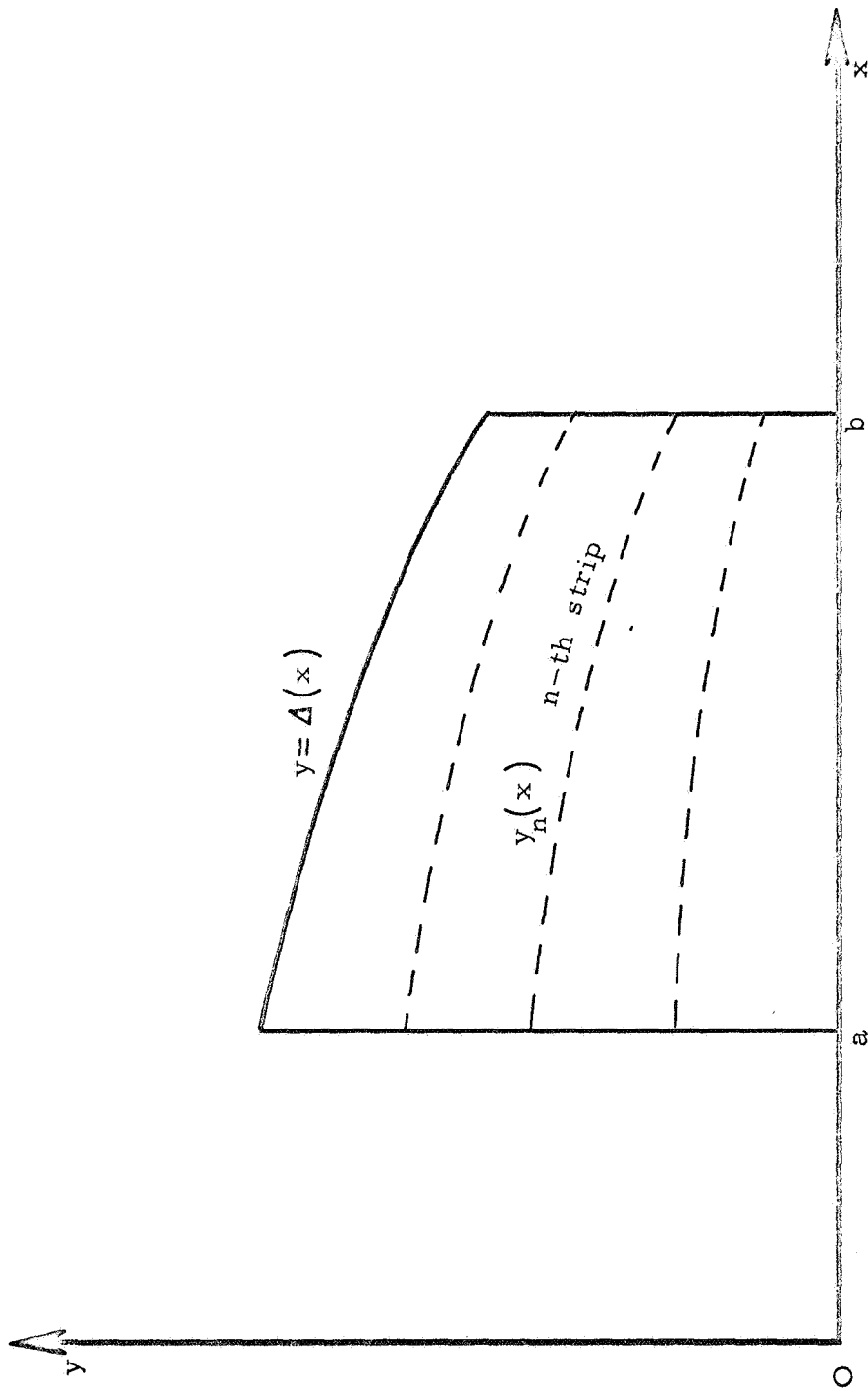


FIG. 4.1 CONSTRUCTION OF THE STRIPS IN THE DOMAIN OF INTEGRATION

$$\left. \begin{array}{l}
\text{at } y = 0 \\
\psi_{\nu}(x, u_1, u_2, \dots, u_L) = 0 \\
\nu = 1, 2, \dots, j \\
\\
\text{at } y = \Delta(x) \\
\psi_{\nu}(x, u_1, u_2, \dots, u_L) = 0 \\
\nu = j+1, j+2, \dots, L
\end{array} \right\} \quad (4.3)$$

If the boundary $y = \Delta(x)$ is not known in advance, then an additional boundary condition must be imposed there, i.e. at $y = \Delta(x)$ the index ν should run from $\nu = j+1$ to $\nu = L+1$. Note also that the conditions (4.2) and (4.3) can be differential relations rather than algebraic or transcendental. If there are singular points on a boundary, the corresponding boundary conditions may be absent; they are then replaced by the condition of regularity of the solution at that singularity. This situation is typical in the blunt body problem.

In the method of integral relations, the solution is constructed in successive approximations. Let us consider the N th approximation. The region of integration is divided into N strips by constructing $N-1$ lines between the boundaries, for example, $y = 0$ and $y = \Delta(x)$ (see Figure 4.1) :

$$y = y_n(x) \quad , \quad n = 0, 1, \dots, N \quad (4.4)$$

where $y_0 = 0$, $y_N(x) = \Delta(x)$. The reader should note that there is no restriction upon the spacing of the lines $y_n(x)$. A common practice is to have them equally spaced, unless emphasis is desired on a certain region of integration.

Next, a system of L groups of N linearly independent "weighting functions" $f_{l,n}(x,y,u_1,u_2,\dots,u_L)$ is chosen

$$\left\{ f_{l,n}(x,y,u_1,u_2,\dots,u_L) \right\} = \left\{ f_{l,1}, \dots, f_{l,N} \right\} \quad (l = 1, 2, \dots, L) \quad (4.5)$$

In the first improvement of the method, Dorodnitsyn [4.6] chose these functions to be only y dependent. Further, Deacon and Oliver [4.13] used them as a function of one of the unknowns u_l .

If the system (4.1) is multiplied by $f_{l,n}$ and integrated between $y_n(x)$ and $y_{n+1}(x)$, one has

$$\int_{y_n}^{y_{n+1}} f_{l,n} \left\{ \frac{\partial P_l}{\partial x} + \frac{\partial Q_l}{\partial y} - F_l \right\} dy = 0 \quad (n = 0, 1, \dots, N), \quad (l = 1, 2, \dots, L) \quad (4.6)$$

or expanding the integrand and taking $f_{l,n}$ only y dependent for simplicity

$$\begin{aligned} \frac{d}{dx} \int_{y_n}^{y_{n+1}} f_{l,n} P_l dy - f_{l,n,n+1} P_{l,n+1} y'_{n+1} + \\ f_{l,n} P_{l,n} y'_n + f_{l,n,n+1} Q_{l,n+1} - f_{l,n,n} Q_{l,n} - \\ \int_{y_n}^{y_{n+1}} Q_l df_{l,n} = \int_{y_n}^{y_{n+1}} f_{l,n} F_l dy \end{aligned} \quad (n = 0, 1, \dots, N), \quad (l = 1, 2, \dots, L) \quad (4.7)$$

If now, for the integrand functions P_l, Q_l, F_l we apply any interpolation formula expressing their values at any y through the values on

the lines $y_n(x)$ and integrate, we shall have

$$\int_{y_n}^{y_{n+1}} f_{l,n} P_l dy = \Delta(x) \sum_{i=0}^N A_{n,i} \Pi_{l,i} \quad (4.8)$$

$$\int_{y_n}^{y_{n+1}} f_{l,n} Q_l dy = \Delta(x) \sum_{i=0}^N B_{n,i} K_{l,i} \quad (4.9)$$

$$\int_{y_n}^{y_{n+1}} f_{l,n} F_l dy = \Delta(x) \sum_{i=0}^N C_{n,i} \Phi_{l,i} \quad (4.10)$$

where in (4.7) $f_{l,n}, P_l, Q_l$ are the functions $f_{l,n}, P_l, Q_l$ evaluated at $y_n(x)$, and in (4.8), (4.9), and (4.10) $A_{n,i}, B_{n,i}, C_{n,i}$ are numerical coefficients whose value depends on the particular choice of $f_{l,n}$ and the interpolating formula for P_l, Q_l , and F_l ; $\Pi_{l,i}, K_{l,i}, \Phi_{l,i}$ are the functions

$$\begin{aligned} \Pi_{l,i} &= \Pi_{l,i} (x, u_{l,0}, u_{l,1}, \dots, u_{l,n}) \\ K_{l,i} &= K_{l,i} (x, u_{l,0}, u_{l,1}, \dots, u_{l,n}) \\ \Phi_{l,i} &= \Phi_{l,i} (x, u_{l,0}, u_{l,1}, \dots, u_{l,n}) \\ & (\quad l = 1, 2, \dots, L \quad) , \quad (\quad i = 0, 1, \dots, N \quad) \end{aligned} \quad (4.11)$$

where $u_{l,m}$ are functions of x to be determined and they are the values of the unknowns u_l at the line $y_m(x)$. Most of the time, these smoothing functions are chosen to be polynomials in y with co-

efficients depending implicitly on x , but very recently Bossel [4.17] has inserted terms of the type $a(x) \exp \{ \alpha(x) y \} y^k$ in boundary layer calculations. With (4.8) to (4.11) the system (4.7) can be written as

$$\sum_{i=0}^N \left\{ A_{n,i} \frac{d}{dx} \left[\Delta(x) \Pi_{\ell,i} \right] - f_{\ell,n,n+1} P_{\ell,n+1} y'_{n+1} + \right. \\ \left. f_{\ell,n,n} P_{\ell,n} y'_n + f_{\ell,n,n+1} Q_{\ell,n+1} - f_{\ell,n,n} Q_{\ell,n} - \right. \\ \left. \Delta(x) \sum_{i=0}^N \left(B_{n,i} K_{\ell,i} \right) = \Delta(x) \sum_{i=0}^N C_{n,i} \Phi_{\ell,i} \right. \\ \left. (n = 0, 1 \dots N) \quad , \quad (\ell = 1, 2 \dots L) \right. \quad (4.12)$$

Equations (4.12) represent a system of $L N$ ordinary differential equations with $(N + 1) L$ unknowns; but from (4.3) one gets the L relations

$$\left. \begin{aligned} \Psi_{\nu} (x, u_{10}, u_{20}, \dots, u_{L0}) &= 0 \\ (\nu = 1, 2 \dots j) \\ \Psi_{\nu} (x, u_{1N}, u_{2N}, \dots, u_{LN}) &= 0 \\ (\nu = j + 2, \dots, L) \end{aligned} \right\} \quad (4.13)$$

by which one can eliminate L unknowns from (4.12).

In the same manner (4.2) yields the new boundary conditions

$$\left. \begin{aligned}
 \text{at } x = a, \varphi_\nu (y_n, \bar{u}_{1n}, \bar{u}_{2n} \dots \bar{u}_{ln}) &= 0 \\
 (\nu = 1, 2 \dots h) \\
 \text{at } x = b, \varphi_\nu (y_n, \bar{\bar{u}}_{1n}, \bar{\bar{u}}_{2n} \dots \bar{\bar{u}}_{ln}) &= 0 \\
 (\nu = h + 1 \dots L)
 \end{aligned} \right\} \quad (4.14)$$

Equations (4.14) are the boundary conditions for system (4.12) and they represent $L (N + 1)$ integral or differential relations between the $L (N + 1)$ unknowns $u_{\mathcal{L},n}$ at the boundaries $x = a$ and $x = b$, i.e. $\bar{u}_{\mathcal{L},n}, \bar{\bar{u}}_{\mathcal{L},n}$, but note that L of them have to be identical to (4.13) for $x = 0$ and therefore one has $L N$ independent conditions to determine the $L N$ constants of integration of the system (4.12).

4.3 Accuracy, Practicability and Convergence

The method of integral relations shows great accuracy for blunt body calculations. For example, the three strip solution for the sphere presented by Belotserkovskii [4.8] is believed to be the most accurate as compared with experiments. The two strip solution for the same case gives very nearly the same accuracy as the three strips. There is not yet a satisfactory explanation of the reason for such accuracy. (It should be noted that the accuracy may be further improved) It could appear that a partial list of reasons for this accuracy is as follows. a) The integration procedure smoothes the irregularities introduced by numerical computations as compared to the schemes used by finite difference methods.

b) The preceding statement is especially true for cases in which singularities are present within the field of integration. In using finite differences the geometry of the mesh has to be changed and diminished around the singularity; no special modification needs to be taken in the method under discussion unless one wants to have improved accuracy in the neighbourhood of the singularity. The reason is that the divergence form of the governing differential equations allows for the integration through the singularity; the conservation laws are thus automatically satisfied.* c) Any knowledge of the qualitative or quantitative nature of the physics of the problem can be introduced into the scheme by choosing appropriate smoothing functions to approximate the integrands occurring in equations (4.7). This flexibility of the method is extremely important for possible increases in the accuracy without corresponding increases in the order of approximation. d) The most striking feature is the remarkable improvement of the method by a convenient choice of the system of weighting functions. It is a fact that if one chooses the right system of functions the accuracy is improved, but there is no explanation for this improvement. There has not been much use of the weighting functions in the blunt body problem, but researchers in boundary layer theory have made wide use of these functions since in boundary layer type problems the region of integration is infinite in the direction normal to the body surface, the use of weighting functions is the only way to generate as many ordinary differential equations as parameters introduced in the approximation of the integrands; however, it would appear that the use of these functions has not been totally exploited as yet. Most of the investigators in boundary

* Except if the physical model breaks down near to the singularity

layer theory have limited themselves to the use of systems of functions that have been shown in the past to give good accuracy for the particular case of the integration of the boundary layer equations; however, Bethel [4.1] has investigated the effect on the accuracy of three different families of weighting functions and found that it is very small for the cases that he studied.

Going back to the general method where the region of integration is finite, one can solve the problem without using any weighting function and determine the introduced parameters by using a convenient number of strips. Suppose now that the system of weighting functions (4.5) has been chosen in such a way that all of them acquire the value zero at the lower boundary of the corresponding strip. Examining equation (4.7), one can see that with a proper choice of $f_{l,n}$ one can compute the integrals (regardless of the choice of the smoothing functions) in such a way that the main contribution to the value of the integral comes from the region of the strip where $f_{l,n}$ has a peak value. Thus the general recommendation for the use of weighting functions is to select them in such a way that they have a peak for the value of the variable arguments around which the profile approximated by the smoothing functions is known to be very accurate. A general disadvantage of the method is that the accuracy depends on the choice of the expression to be approximated by the smoothing functions as well as the particular system of coordinates. A general rule for that option is to examine previous experience on similar cases and to take them as a basis of comparison. There has not been developed, as yet, a study of the scheme for the linear differential equations, but

it would appear that one could learn much of the effects described above on the accuracy of the different order of approximation by carrying out computations for the non-linear case similar to those that have been proved to be successful in the linear case.

With regard to the practicability, it should be said that the fact that the problem has been reduced to the integration of a system of ordinary differential equations makes it plausible to apply the well known and well developed finite difference techniques. However, beyond the first approximation, the formulation of the method becomes very tedious and requires lengthy transformations and algebra; there is, on the other hand, an advantage of the method in that these transformations are purely mechanical, and, although it has not been demonstrated yet, they can be handled by a program written in "FORMAC"* (an extension of PL/I compiler); this procedure is presently being applied to boundary layer problems.** This is especially feasible for cases like the present one in which the governing differential equations are quasi-linear, making it possible by elemental means to find explicitly the derivatives as a function of the independent and dependent variables. Once the analytic expressions of the system of ordinary differential equations is known, it is quite practical to develop a code for an electronic machine to solve this system without over-loading the memory of the machine by using subroutines for the different steps of the code. There are, however, some special cases with peculiar boundary conditions that require careful treatment, thus enlarging the

* See Reference [4.18]

** N. Mitra and H. Bossel, private communication

size of the program (for example, the blunt body problem with a discontinuity on the body).

The convergence of the solution as the number of strips increases is totally unknown due to the fact that the blunt body problem has not been carried out for more than three strips. Therefore, one does not know whether the solution gets better for higher N or if there is a certain value of N beyond which the solution diverges from the true solution, that is, the method would give an asymptotic expansion rather than the terms of a convergent series expansion. There have been some efforts in boundary layer theory to investigate the convergence of the method when applied in a particular version (Bethel [4.1]). However, there are cases in which special care needs to be taken or the solution diverges for very high N , for example, the blunt body problem with a shock within the region of integration in which a step function is being approximated by polynomials. In general one can say that there is nothing to assure convergence and that a special study for each case may be necessary.

5. APPLICATION OF THE METHOD OF INTEGRAL RELATIONS TO THE CASE OF A BLUNT BODY IN A NON-UNIFORM FLOW

5.1 Introduction

In the present section the method of integral relations is applied in its first approximation to the case of the blunt body under the conditions described in earlier sections.

A feature of the integral relation hypersonic flow field solutions of the blunt body problem is that a one strip approximation usually gives quite accurate results (see reference [5.1]) when applied according to Scheme 1,^{*} i.e., taking the strips parallel to the body surface. In our case, however, one has to be cautious about the reliability of the numerical results because the influence of the non-uniformities upstream in the shock wave may considerably reduce the accuracy of the method. Thus, the results of this numerical scheme will be significant only from a qualitative point of view, and for more reliable numerical results it is recommended that one applies the second or if possible the third approximation.

The same notation that was used in Section 3 will be followed in the present section, except as otherwise specified. The formulation will be developed for a body of revolution whose meridian curve is of the most general geometrical shape.

5.2 Formulation

The flow equations utilized are the continuity equation, the n-momentum equation, Bernoulli's equation or the energy equation along

* i.e., the case in which the strips are taken parallel to the body

a streamline and the conservation of entropy along a trajectory, or i.e., along a streamline in a steady flow.

The equations of continuity and n-momentum were derived in section 3 and they are given here again for convenience

$$\frac{\partial T}{\partial s} - \xi \frac{\partial}{\partial \xi} \left(\frac{\epsilon'}{\epsilon} T \right) + \frac{\partial}{\partial \xi} \left(\frac{A L}{\epsilon} \right) = 0 \quad (5.1)$$

$$\frac{\partial Z}{\partial s} - \xi \frac{\partial}{\partial \xi} \left(\frac{\epsilon'}{\epsilon} Z \right) + \frac{\partial}{\partial \xi} \left(\frac{A H}{\epsilon} \right) = Y \quad (5.2)$$

$$T = \rho v y \quad (5.3)$$

$$A = 1 + \frac{n}{R} \quad (5.4)$$

$$L = \rho u y \quad (5.5)$$

$$Z = \rho u v y \quad (5.6)$$

$$H = y (p + \rho u^2) \quad (5.7)$$

$$Y = \frac{G}{R} + A p \sin \theta \quad (5.8)$$

$$G = y (p + \rho v^2) \quad (5.9)$$

$R =$ radius of curvature of the body

In the analysis which follows, suffix 0 refers to conditions on the body while suffix 1 refers to conditions immediately behind the shock. The distance of a general point from the axis of symmetry is given by

$$y = y_0(s) + n \sin \theta \quad (5.10)$$

To apply the method of integral relations in the first approximation, interpolate linearly for T , Z , and Y between the body and the shock using the formulae

$$T = T_0 + (T_1 - T_0) \xi \quad (5.11)$$

$$Z = Z_0 + (Z_1 - Z_0) \xi \quad (5.12)$$

$$Y = Y_0 + (Y_1 - Y_0) \xi \quad (5.13)$$

Then substitute in (5.1) and (5.2) and integrate with respect to ξ from 0 to 1. We obtain the relations

$$\begin{aligned} \frac{d}{ds} \left[\frac{1}{2} (T_0 + T_1) \right] - \frac{\epsilon'}{\epsilon} T_1 + \\ \frac{\epsilon'}{\epsilon} \frac{1}{2} (T_0 + T_1) + \frac{A_1 L_1 - A_0 L_0}{\epsilon} = 0 \end{aligned} \quad (5.14)$$

$$\begin{aligned} \frac{d}{ds} \left[\frac{1}{2} (Z_0 + Z_1) \right] - \frac{\epsilon'}{\epsilon} Z_1 + \frac{\epsilon'}{\epsilon} \frac{1}{2} (Z_0 + Z_1) + \\ \frac{A_1 H_1 - A_0 H_0}{\epsilon} = \frac{1}{2} (Y_1 + Y_0) \end{aligned} \quad (5.15)$$

These may be written as

$$T_1' = -T_0' + \frac{\epsilon'}{\epsilon} (T_1 - T_0) - \frac{2}{\epsilon} (A_1 L_1 - A_0 L_0) \quad (5.16)$$

$$Z_1' = \frac{\epsilon'}{\epsilon} Z_1 - \frac{2}{\epsilon} (A_1 H_1 - A_0 H_0) + Y_1 + Y_0 \quad (5.17)$$

since $Z_0' = Z_0 = 0$.

The differential equations (5.16) and (5.17) can be expressed entirely in terms of the dependent variables ϵ , σ , and v_0 .

The differential equation for ϵ is given by the geometrical relation

$$\frac{d\epsilon}{ds} = A_1 \tan(\beta - \alpha) \quad (5.18)$$

where

$$\beta = \frac{\pi}{2} - \sigma \quad (5.19)$$

$$\alpha = \frac{\pi}{2} - \theta \quad (5.20)$$

The differential equation for v_o is derived from the definition

$$T_o = \rho_o v_o y_o \quad (5.21)$$

Then

$$T_o' = y_o' \rho_o v_o + y_o \rho_o' v_o + y_o \rho_o v_o' \quad (5.22)$$

Since the body surface is a streamline, we know from the Bernoulli equation that

$$dp_o = -\rho_o v_o dv_o \quad (5.23)$$

and from the entropy equation that

$$dS_o = 0 \quad (5.24)$$

The speed of the sound is thus

$$a_o^2 = \frac{dp_o}{d\rho_o} \quad (5.25)$$

Combining these equations, we obtain the equation

$$dp_o = - \frac{\rho_o v_o}{a_o^2} dv_o \quad (5.26)$$

If (5.26) is substituted in (5.22) the differential equation for v_o is given as

$$v_o' = \frac{T_o' - y_o' \rho_o v_o}{y_o' \rho_o \left(1 - \frac{v_o^2}{a_o^2}\right)} \quad (5.27)$$

where y_o' is specified by the body geometry, and the speed of the sound, a_o , on the body streamline is given by the Bernoulli equation in the form

$$a_o^2 = \frac{\gamma-1}{2} (1 - v_o^2) \quad (5.28)$$

The density ρ_o and pressure p_o are found as a function of v_o with the help of the equation of conservation of the entropy along a streamline and they are

$$\rho_o = \left(\frac{\gamma-1}{2\gamma}\right)^{\frac{1}{\gamma-1}} (1 - v_o^2)^{\frac{1}{\gamma-1}} \varphi_i^{-\frac{1}{\gamma-1}} \quad (5.29)$$

$$p_o = \left(\frac{\gamma-1}{2\gamma}\right)^{\frac{\gamma}{\gamma-1}} (1 - v_o^2)^{\frac{\gamma}{\gamma-1}} \varphi_i^{-\frac{1}{\gamma-1}} \quad (5.30)$$

where φ_i is given by

$$\varphi_i = \frac{p_i}{\rho_i \gamma} \quad (5.31)$$

p_i and ρ_i are the pressure and density behind the shock at the center line and they are given by the shock jump relations (3.31) and (3.32) for the case $\sigma = 0$. T'_0 is determined by the continuity integral relation differential equation (5.16) by

$$T'_0 = -T'_1 + \frac{\epsilon'}{\epsilon} (T'_1 - T'_0) - \frac{2}{\epsilon} (A_1 L_1 - A_0 L_1) \quad (5.32)$$

To evaluate T'_1 , we utilize the definition

$$T_1 = y_1 \rho_1 v_1 \quad (5.33)$$

Then

$$T'_1 = y'_1 \rho_1 v_1 + y_1 v_1 \rho'_1 + y_1 \rho_1 v'_1 \quad (5.34)$$

where

$$\rho'_1 = \frac{\partial \rho_1}{\partial \beta} \frac{\partial \beta}{\partial s} + \frac{\partial \rho_1}{\partial y_1} y'_1 \quad (5.35)$$

$$y'_1 = y'_0 + \cos \alpha \frac{d\epsilon}{ds} + \frac{\epsilon}{R} \sin \alpha \quad (5.36)$$

v'_1 is defined later in equation (5.46). The final form of the equation is then

$$\frac{dv_0}{ds} = \frac{E_0}{F_0} \quad (5.37)$$

with

$$E_o = \frac{(T_o' - y_o' \rho_o v_o') a_o^2}{y_o' \rho_o} \quad (5.38)$$

and

$$F_o = a_o^2 - v_o^2 \quad (5.39)$$

In the present system of coordinates, the differential equation for β can be deduced from the n-momentum integral relation differential equation (5.17) and the shock boundary conditions. From the definition of Z_1 one has

$$Z_1' = \rho_1 u_1 v_1 y_1' + y_1 (\rho_1 u_1 v_1)' \quad (5.40)$$

where y_1' is given by equation (5.36). At this point it is convenient to introduce the equations relating the boundary layer coordinate velocity components to the velocity components q_t, q_n , tangential and normal to the shock. Thus

$$u_1 = q_t \sin(\beta - \alpha) - q_n \cos(\beta - \alpha) \quad (5.41)$$

$$v_1 = q_t \cos(\beta - \alpha) + q_n \sin(\beta - \alpha) \quad (5.42)$$

The conditions across the shock are given by

Continuity

$$\rho_1 q_n = \rho_\infty q_\infty \sin \beta \quad (5.43)$$

Tangential momentum

$$q_t = q_\infty \cos \beta \quad (5.44)$$

and one gets

$$\frac{du_1}{ds} = U_1 \frac{d\beta}{ds} + U_2 \frac{dy_1}{ds} - v_1 \frac{d\alpha}{ds} \quad (5.45)$$

$$\frac{dv_1}{ds} = V_1 \frac{d\beta}{ds} + V_2 \frac{dy_1}{ds} + u_1 \frac{d\alpha}{ds} \quad (5.46)$$

where

$$U_1 = \frac{\partial q_t}{\partial \beta} \sin (\beta - \alpha) - \frac{\partial q_n}{\partial \beta} \cos (\beta - \alpha) + v_1 \quad (5.47)$$

$$V_1 = \frac{\partial q_t}{\partial \beta} \cos (\beta - \alpha) + \frac{\partial q_n}{\partial \beta} \sin (\beta - \alpha) - u_1 \quad (5.48)$$

$$U_2 = \frac{\partial q_t}{\partial y_1} \sin (\beta - \alpha) - \frac{\partial q_n}{\partial y_1} \cos (\beta - \alpha) \quad (5.49)$$

$$V_2 = \frac{\partial q_t}{\partial y_1} \cos (\beta - \alpha) + \frac{\partial q_n}{\partial y_1} \sin (\beta - \alpha) \quad (5.50)$$

$$\frac{\partial q_t}{\partial \beta} = -q_\infty \sin \beta \quad (5.51)$$

$$\frac{\partial q_n}{\partial \beta} = \frac{\rho_\infty q_\infty}{\rho_1} \cos \beta + q_\infty \sin \beta \frac{\partial}{\partial \beta} \left(\frac{\rho_\infty}{\rho_1} \right) \quad (5.52)$$

$$\frac{\partial q_t}{\partial y_1} = \cos \beta \frac{dq_\infty}{dy_1} \quad (5.53)$$

$$\frac{\partial q_n}{\partial y_1} = \sin \beta \frac{\partial}{\partial y_1} \left(\frac{\rho_\infty q_\infty}{\rho_1} \right) \quad (5.54)$$

$$\frac{dp_\infty}{dy_1} = - \frac{\gamma-1}{2} \left(1 + \frac{\gamma-1}{2} M_\infty^2 \right)^{-\frac{2\gamma-1}{\gamma-1}} M_\infty \frac{dM_\infty}{dy_1} \quad (5.55)$$

$$\frac{dq_\infty}{dy_1} = \frac{\frac{\gamma-1}{2} M_\infty f^2}{\left(1 + \frac{\gamma-1}{2} M_\infty^2 \right)^2 q_\infty} \frac{dM_\infty}{dy} + \frac{q_\infty}{f} \frac{df}{dy_1} \quad (5.56)$$

and from (3.32)

$$\frac{\partial}{\partial y_1} \left(\frac{\rho_\infty}{\rho_1} \right) = - \frac{4}{(\gamma+1) \sin^2 \beta M_\infty^3} \frac{dM_\infty}{dy_1} \quad (5.57)$$

$$\frac{\partial}{\partial \beta} \left(\frac{\rho_\infty}{\rho_1} \right) = - \frac{2 \sin 2 \beta}{(\gamma+1) \sin^4 \beta M_\infty^2} \quad (5.58)$$

For ρ_1' one gets

$$\frac{d\rho_1}{ds} = \frac{\partial\rho_1}{\partial\beta} \frac{d\beta}{ds} + \frac{\partial\rho_1}{\partial y_1} \frac{dy_1}{ds} \quad (5.59)$$

where

$$\frac{\partial\rho_1}{\partial\beta} = -\frac{\rho_1^2}{\rho_\infty} \frac{\partial}{\partial\beta} \left(\frac{\rho_\infty}{\rho_1} \right) \quad (5.60)$$

$$\frac{\partial\rho_1}{\partial y_1} = \frac{\rho_1}{\rho_\infty} \frac{d\rho_\infty}{dy_1} - \frac{\rho_1^2}{\rho_\infty} \frac{\partial}{\partial y_1} \left(\frac{\rho_\infty}{\rho_1} \right) \quad (5.61)$$

and

$$\frac{d\rho_\infty}{dy_1} = -\frac{4\gamma}{\gamma-1} \frac{f(y_1) \frac{df}{dy_1} - q_\infty \frac{dq_\infty}{dy_1}}{[f(y_1)^2 - q_\infty^2]^2} \rho_\infty + \frac{\rho_\infty}{\rho_\infty} \frac{d\rho_\infty}{dy_1} \quad (5.62)$$

The last equation follows from (3.42). Going back to equation (5.40)

and substituting u_1' , v_1' and ρ_1' by its expressions one has

$$\begin{aligned} z_1' = & \rho_1 u_1 v_1 \frac{dy_1}{ds} + y_1 \left[u_1 v_1 \left(\frac{\partial\rho_1}{\partial\beta} \frac{d\beta}{ds} + \right. \right. \\ & \left. \left. \frac{\partial\rho_1}{\partial y_1} \frac{dy_1}{ds} \right) + \rho_1 u_1 \left(v_1 \frac{d\beta}{ds} + v_2 \frac{dy_1}{ds} \right) + \right. \\ & \left. \rho_1 v_1 \left(u_1 \frac{d\beta}{ds} + u_2 \frac{dy_1}{ds} \right) + \rho_1 v_1^2 \frac{1}{R} - \right. \\ & \left. \rho_1 u_1^2 \frac{1}{R} \right] \quad (5.63) \end{aligned}$$

and solving (5.63) for $\frac{d\beta}{ds}$, we find that

$$\frac{d\beta}{ds} = \frac{C_1}{B_1} \quad (5.64)$$

with

$$C_1 = Z_1' - \rho_1 u_1 v_1 \frac{dy_1}{ds} - y_1 \left[\frac{\rho_1}{R} (v_1^2 - u_1^2) + u_1 v_1 \frac{\partial \rho_1}{\partial y_1} \frac{dy_1}{ds} + \rho_1 u_1 v_2 \frac{dy_1}{ds} + \rho_1 v_1 U_2 \frac{dy_1}{ds} \right] \quad (5.65)$$

and Z_1' is given by the integral relation equation (5.17)

$$B_1 = y_1 \left[u_1 v_1 \frac{\partial \rho_1}{\partial \beta} + \rho_1 u_1 v_1 + \rho_1 v_1 U_1 \right] \quad (5.66)$$

5.3 Study of the Fixed Singularity

An examination of equations (5.37) and (5.64) shows that they present a singularity at the axis, i.e. for $s = 0$, they are indeterminate.

Equation (5.64), when $s = 0$, is written as

$$\frac{d\beta}{ds} = \frac{C_1}{B_1} \quad (5.67)$$

where again the primed quantities denote differentiation with respect to the arc length s . Since for $s = 0$ one should recall that the symmetry of the distributions of Mach number and total energy in the free flow makes

$$\frac{dM_\infty}{dy_1} = \frac{df(y_1)}{dy_1} = 0 \quad (5.68)$$

and consequently

$$V_2 = U_2 = 0 \quad (5.69)$$

and from the non-dimensionalization of the lengths by the radius of curvature of the body at the center line, $R_{s=0} = 1$, then from equation (5.65), when $s \rightarrow 0$, one gets

$$C_1' = Z_1'' - A_1 \rho_1 u_1 V_1 + 2 A_1 \rho_1 u_1^2 \quad (5.70)$$

From (5.66)

$$B_1' = A_1 \rho_1 u_1 V_1 \quad (5.71)$$

Hence, when $s \rightarrow 0$

$$\frac{d\beta}{ds} = \frac{Z_1'' + 2 A_1 \rho_1 u_1^2}{2 \rho_1 u_1 V_1 A_1} \quad (5.72)$$

In order to determine Z_1'' we go back to equation (5.17) to get

$$Z_1'' = -\frac{2}{e} (A_1 H_1)' - (A_0 H_0)' + Y_1' + Y_0' \quad (5.73)$$

because for $s = 0$, $Z_1' = 0$. But for this value of s one has also

$$(A_1 H_1)' = A_1^2 (p_1 + \rho_1 u_1^2) \quad (5.74)$$

$$(A_0 H_0) = p_0 \quad (5.75)$$

$$Y_1' = 2 A_1 p_1 \quad (5.76)$$

$$Y_0' = 2 p_0 \quad (5.77)$$

Hence

$$Z_1'' = -\frac{2}{\epsilon} \left[A_1^2 (p_1 + \rho_1 u_1^2) - p_0 \right] + 2 (A_1 p_1 + p_0) \quad (5.78)$$

In the same way, equation (5.38) for $s \rightarrow 0$ can be written as

$$E_0 = \left[\frac{T_0''}{\rho_0} - v_0' \right] a_0^2 \quad (5.79)$$

To evaluate T_0'' we use equation (5.16). When $s \rightarrow 0$ we have

$$T_0'' = -T_1'' - \frac{2}{\epsilon} (A_1 L_1)' \quad (5.80)$$

and if one computes the derivatives by a limiting procedure as $s \rightarrow 0$

we have

$$-T_0'' = T_1'' + \frac{2 A_1^2 \rho_1 u_1}{\epsilon} \quad (5.81)$$

Now when $s = 0$

$$T_1'' = \frac{Z_1''}{u_1} \quad (5.82)$$

where Z_1'' is determined from equation (5.78). Therefore one has finally

$$\frac{dv_0}{ds} = \frac{T_0''}{2 \rho_0} \quad (5.83)$$

The initial values of the variables and their derivatives are thus

$$\begin{aligned} s &= 0 \\ \epsilon &= \epsilon_i \\ \beta &= \frac{\pi}{2} \\ v_0 &= 0 \\ \epsilon' &= 0 \\ \beta' &= \text{given by equation (5.72)} \\ v_0' &= \text{given by equation (5.83)} \end{aligned} \quad (5.84)$$

5.4 Moving Singularity

It is obvious that equation (5.37) presents a singularity for the value of s corresponding to the point on the body for which $v_0 = a_0$ i.e. for the sonic point on the body. This is a feature of the method and it occurs also for the cases of higher approximations. This point has been fully studied by Belotserkovskii (see reference [5.2]) and it has been shown to be a singular point of the saddle type. The condition of regularity of the solution at this point imposes an extra condition to determine the stand-off distance at the axis ϵ_i that up to now was undetermined. In the next section the mathematical

procedure to determine ϵ_1 is given as well as the method to pass through the singular point in order to find the solution for values of s larger than the one that corresponds to the sonic point, i.e. the saddle point.

5.5 Shock Layer Properties.

The formulation expressed in the preceding paragraphs reduces the problem to the integration of a system of ordinary differential equations that gives ϵ , β , v_0 as a function of s . In order to determine the rest of the flow field variables as well as their distribution across the shock layer one should proceed as follows: with the help of equations (5.3), (5.6), and (5.8) one computes Z , T , and Y for the body surface and for the shock. Since Z and T vary linearly across the shock, one has directly (the numbers refer to the steps in the iterative sequence)

$$1) \quad u(s, \xi) = \frac{Z_0 + (Z_1 - Z_0) \xi}{T_0 + (T_1 - T_0) \xi} \quad (5.85)$$

2) Assume a value for $v(s, \xi)$ given by

$$v(s, \xi) = v_0 + (v_1 - v_0) \xi \quad (5.86)$$

With this value of v substitute in

$$T = \gamma \rho v \quad (5.87)$$

and

$$Y = \frac{\gamma (p + \rho v^2)}{R} + A p \cos \alpha \quad (5.88)$$

to get p and ρ as a function of s and ξ

- 3) From the energy equation compute $f(y_{1s})$ where y_{1s} refers to the point of intersection of the shock and the streamline that passes through the point (s, ξ)

$$f(y_{1s})^2 = \left(\frac{1}{2} q^2 + \frac{\gamma}{\gamma-1} \frac{p}{\rho} \right)^2 \quad (5.89)$$

- 4) Compute the corresponding $\varphi(y_{1s})$ and find p such that

$$p = \rho^\gamma \varphi(y_{1s}) \quad (5.90)$$

- 5) With this value of p compute from (5.88) a new v and repeat the process again until the desired accuracy is reached.

5.6 Summary of Formulae

For convenience and clarity the necessary formulae for the computation of the flow field variables are given in the order that would appear in a code for a computer

$$\underline{s = 0}$$

$$q_{\infty i} = \left[\frac{\frac{\gamma-1}{2} M_{\infty i}^2}{1 + \frac{\gamma-1}{2} M_{\infty i}^2} \right]^{\frac{1}{2}} \quad (5.91)$$

$$p_{1i} = \left[1 + \frac{2\gamma}{\gamma+1} (M_{\infty i}^2 - 1) \right] p_{\infty i} \quad (5.92)$$

$$\rho_{\infty i} = \frac{\frac{2}{\gamma-1}}{1 - q_{\infty i}^2} p_{\infty i} \quad (5.93)$$

$$\rho_{1i} = \rho_{\infty i} \frac{(\gamma + 1) M_{\infty i}^2}{(\gamma - 1) M_{\infty i}^2 + 2} \quad (5.94)$$

$$\varphi_i = p_{1i} \rho_{1i}^{-\gamma} \quad (5.95)$$

$$\rho_{oi} = \left(\frac{\gamma-1}{2\gamma} \right)^{\frac{1}{\gamma-1}} \varphi_i^{-\frac{1}{\gamma-1}} \quad (5.96)$$

$$p_{oi} = \rho_{oi} \frac{\gamma-1}{2\gamma} \quad (5.97)$$

$$q_{ni} = q_{\infty i} \frac{\rho_{\infty i}}{\rho_{1i}} \quad (5.98)$$

$$A_{1i} = 1 + \epsilon_i \quad (5.99)$$

$$V_{1i} = -q_{\infty i} + q_{ni} \quad (5.100)$$

$$Z_{1i}'' = -\frac{2}{\epsilon_i} \left[A_{1i}^2 (p_{1i} + \rho_{1i} q_{ni}^2) - p_{oi} \right] + 2 (A_{1i} p_{1i} + p_{oi}) \quad (5.101)$$

$$T_{oi}'' = \frac{Z_{1i}''}{q_{ni}} + \frac{2 A_{1i}^2 \rho_{1i} q_{ni}}{\epsilon_i} \quad (5.102)$$

$$\left(\frac{d\epsilon}{ds} \right)_i = 0 \quad (5.103)$$

$$\left(\frac{d\beta}{ds} \right)_i = -\frac{Z_{1i}'' + 2 A_{1i} \rho_{1i} q_{ni}^2}{2 \rho_{1i} q_{ni} V_{1i} A_{1i}} \quad (5.104)$$

$$\frac{dv_o}{ds} \Big|_i = \frac{T_o''}{2 \rho_{oi}} \quad (5.105)$$

s > 0

$$\frac{de}{ds} = (1 + e) \tan(\beta - \alpha) \quad (5.106)$$

$$q_\infty = \left[\frac{\frac{\gamma-1}{2} M_\infty^2}{1 + \frac{\gamma-1}{2} M_\infty^2} \right]^{\frac{1}{2}} f(y_1) \quad (5.107)$$

$$\rho_\infty = \frac{\frac{2\gamma}{\gamma-1}}{f(y)^2 - q_\infty^2} p_\infty \quad (5.108)$$

$$\rho_1 = \rho_\infty \frac{(\gamma + 1) M_\infty^2 \sin^2 \beta}{(\gamma - 1) M_\infty^2 \sin^2 \beta + 2} \quad (5.109)$$

$$p_1 = \left[1 + \frac{2\gamma}{\gamma+1} (M_\infty^2 \sin^2 \beta - 1) \right] p_\infty \quad (5.110)$$

$$q_t = q_\infty \cos \beta \quad (5.111)$$

$$q_n = \frac{\rho_\infty}{\rho_1} q_\infty \sin \beta \quad (5.112)$$

$$\frac{\partial}{\partial y_1} \left(\frac{\rho_\infty}{\rho_1} \right) = - \frac{4}{(\gamma + 1) \sin^2 \beta M_\infty^3} \frac{dM_\infty}{dy_1} \quad (5.113)$$

$$\frac{\partial}{\partial \beta} \left(\frac{\rho_\infty}{\rho_1} \right) = - \frac{2 \sin 2\beta}{(\gamma + 1) \sin^4 \beta M_\infty^2} \quad (5.114)$$

$$\frac{dq_\infty}{dy_1} = \frac{\frac{\gamma-1}{2} M_\infty^2 r^2}{\left(1 + \frac{\gamma-1}{2} M_\infty^2\right)^2} \frac{dM_\infty}{dy} + \frac{q_\infty}{r} \frac{df}{dy_1} \quad (5.115)$$

$$\frac{\partial q_t}{\partial y_1} = \cos \beta \frac{dq_\infty}{dy_1} \quad (5.116)$$

$$\frac{\partial q_t}{\partial \beta} = -q_\infty \sin \beta \quad (5.117)$$

$$\frac{\partial q_n}{\partial \beta} = \frac{\rho_\infty q_\infty}{\rho_1} \cos \beta + q_\infty \sin \beta \frac{\partial}{\partial \beta} \left(\frac{\rho_\infty}{\rho_1} \right) \quad (5.118)$$

$$\frac{\partial q_n}{\partial y_1} = \sin \beta \left[\frac{\rho_\infty}{\rho_1} \frac{dq_\infty}{dy_1} + q_\infty \frac{\partial}{\partial y_1} \left(\frac{\rho_\infty}{\rho_1} \right) \right] \quad (5.119)$$

$$\frac{dp_\infty}{dy_1} = -\frac{4\gamma}{\gamma-1} \frac{f(y_1) \frac{df}{dy_1} - q_\infty \frac{dq_\infty}{dy_1}}{\left[f(y_1)^2 - q_\infty^2 \right]^2} p_\infty + \frac{\rho_\infty}{p_\infty} \frac{dp_\infty}{dy_1} \quad (5.120)$$

$$\frac{\partial \rho_1}{\partial \beta} = -\frac{\rho_1^2}{\rho_\infty} \frac{\partial}{\partial \beta} \left(\frac{\rho_\infty}{\rho_1} \right) \quad (5.121)$$

$$\frac{\partial \rho_1}{\partial y_1} = \frac{\rho_1}{\rho_\infty} \frac{d\rho_\infty}{dy_1} - \frac{\rho_1^2}{\rho_\infty} \frac{\partial}{\partial y_1} \left(\frac{\rho_\infty}{\rho_1} \right) \quad (5.122)$$

$$\frac{dy_1}{ds} = \frac{dy_0}{ds} + \cos \alpha \frac{d\epsilon}{ds} + \frac{\epsilon}{R} \sin \alpha \quad (5.123)$$

$$\frac{d\rho_1}{ds} = \frac{\partial \rho_1}{\partial \beta} \frac{d\beta}{ds} + \frac{\partial \rho_1}{\partial y_1} \frac{dy_1}{ds} \quad (5.124)$$

$$u_1 = q_t \sin(\beta - \alpha) - q_n \cos(\beta - \alpha) \quad (5.125)$$

$$v_1 = q_t \cos(\beta - \alpha) + q_n \sin(\beta - \alpha) \quad (5.126)$$

$$U_1 = \frac{\partial q_t}{\partial \beta} \sin(\beta - \alpha) - \frac{\partial q_n}{\partial \beta} \cos(\beta - \alpha) + v_1 \quad (5.127)$$

$$V_1 = \frac{\partial q_t}{\partial \beta} \cos(\beta - \alpha) + \frac{\partial q_n}{\partial \beta} \sin(\beta - \alpha) - u_1 \quad (5.128)$$

$$U_2 = \frac{\partial q_t}{\partial y_1} \sin(\beta - \alpha) - \frac{\partial q_n}{\partial y_1} \cos(\beta - \alpha) \quad (5.129)$$

$$V_2 = \frac{\partial q_t}{\partial y_1} \cos(\beta - \alpha) + \frac{\partial q_n}{\partial y_1} \sin(\beta - \alpha) \quad (5.130)$$

$$\frac{du_1}{ds} = U_1 \frac{d\beta}{ds} + U_2 \frac{dy_1}{ds} + \frac{v_1}{R} \quad (5.131)$$

$$\frac{dv_1}{ds} = V_1 \frac{d\beta}{ds} + V_2 \frac{dy_1}{ds} - \frac{u_1}{R} \quad (5.132)$$

$$\rho_o = \left(\frac{\gamma-1}{2\gamma} \right)^{\frac{1}{\gamma-1}} (1 - v_o^2)^{\frac{1}{\gamma-1}} \varphi_i^{-\frac{1}{\gamma-1}} \quad (5.133)$$

$$\rho_o = \left(\frac{\gamma-1}{2\gamma} \right)^{\frac{1}{\gamma-1}} (1 - v_o^2)^{\frac{1}{\gamma-1}} \varphi_i^{-\frac{1}{\gamma-1}} \quad (5.134)$$

$$Z_1' = \frac{1}{\epsilon} \frac{d\epsilon}{ds} Z_1 - \frac{2}{\epsilon} (A_1 H_1 - A_o H_o) + Y_1 + Y_o \quad (5.135)$$

$$T_1' = y_1' \rho_1 v_1 + y_1 v_1 \rho_1' + y_1 \rho_1 v_1' \quad (5.136)$$

$$T_0' = -T_1' + \frac{\epsilon'}{\epsilon} (T_1 - T_0) - \frac{2}{\epsilon} A_1 L_1 \quad (6.137)$$

$$a_0^2 = \frac{\gamma-1}{2} (1 - v_0^2) \quad (5.138)$$

$$E_0 = \frac{(T_0' - y_0' \rho_0 v_0)}{y_0 \rho_0} a_0^2 \quad (5.139)$$

$$F_0 = a_0^2 - v_0^2 \quad (5.140)$$

$$\frac{dv_0}{ds} = \frac{E_0}{F_0} \quad (5.141)$$

$$C_1 = z_1' - \rho_1 u_1 v_1 y_1' - y_1 \left[\frac{\rho_1}{R} (v_1^2 - u_1^2) + y_1' \left(u_1 v_1 \frac{\partial \rho_1}{\partial y_1} + \rho_1 u_1 v_2 + \rho_1 v_1 u_2 \right) \right] \quad (5.142)$$

$$B_1 = y_1 \left(u_1 v_1 \frac{\partial \rho_1}{\partial \beta} + \rho_1 u_1 v_1 + \rho_1 v_1 u_1 \right) \quad (5.143)$$

$$\frac{d\beta}{ds} = \frac{C_1}{B_1} \quad (5.144)$$

5.7 Numerical Procedure

The calculations described in the last paragraph were carried out for a sphere under different conditions described in next section.

In order to integrate the system of ordinary differential equations developed in the last section, the Runge-Kutta method modified by Gill was used.

It should be recalled that the initial stand-off distance of the shock wave had to be attained by satisfying the condition of regularity at the singular point. Following Belotserkovskii's recommendations [5.2] the original procedure for finding the correct solutions on smooth contours has been considerably simplified. Previously it was necessary to stop a given integration ahead of the sonic point and extrapolate the solution up to that point by means of a series expansion. These took time and labor to construct and had to be evaluated for each choice of detachment distance until that corresponding to correct saddle point conditions at the sonic point had been determined. Under the revised procedure, as applied to the first approximation, the integration corresponding to each detachment distance is continued until either the velocity derivative changes in sign or until it attains the value unity. The desired integration always lies between those satisfying these two conditions so that progressively closer upper and lower bounds on the stand-off distance can be found. No extrapolations and series expansions are required to carry out the new scheme if one is only interested in the initial stand-off distance, the distribution of velocity on the body and the shock shape. However, if

the properties across the shock layer are desired, an extrapolation may be necessary in the way described in the next paragraphs.

A general feature of transonic flows is that in the proximity of the sonic line a saddle point in the family of integral curves of any field property appears. A very descriptive example can be seen in the curves for different critical sections A^* that appears in the analysis of a supersonic nozzle. (See for example Liepmann and Roshko [5.3]). The same phenomenon appears in our calculations, and with no further comments we proceed to its analysis.

Assume that an integration of the system of ordinary differential equations is possible for each value of the initial detachment distance ϵ_i . If ϵ_{iex} is the exact value of ϵ_i that makes the solution regular at the sonic point, one would have the pattern of curves sketched in Figure 5.1. In practice it is not possible to carry out the above because the Runge-Kutta scheme becomes unstable before the sonic point is reached. This instability does not appear until the velocity derivative dv_p/ds reaches the value unity if $\epsilon_i < \epsilon_{iex}$ or zero if $\epsilon_i > \epsilon_{iex}$. Therefore, one is able to construct the curves as close as necessary to the regular solution. It has been shown that the location of the points where the velocity derivative for the lower and upper bounds of ϵ_{iex} diverges significantly is very sensitive to the assumed value of ϵ_i and one has to approximate ϵ_{iex} within the sixth significant decimal digit in order to have satisfactory results. For such a purpose, the Runge-Kutta scheme has to be carried with an accuracy larger than 0.000001 and thus the procedure for computing ϵ_{iex} is perhaps longer than it would appear from a superficial inspection.

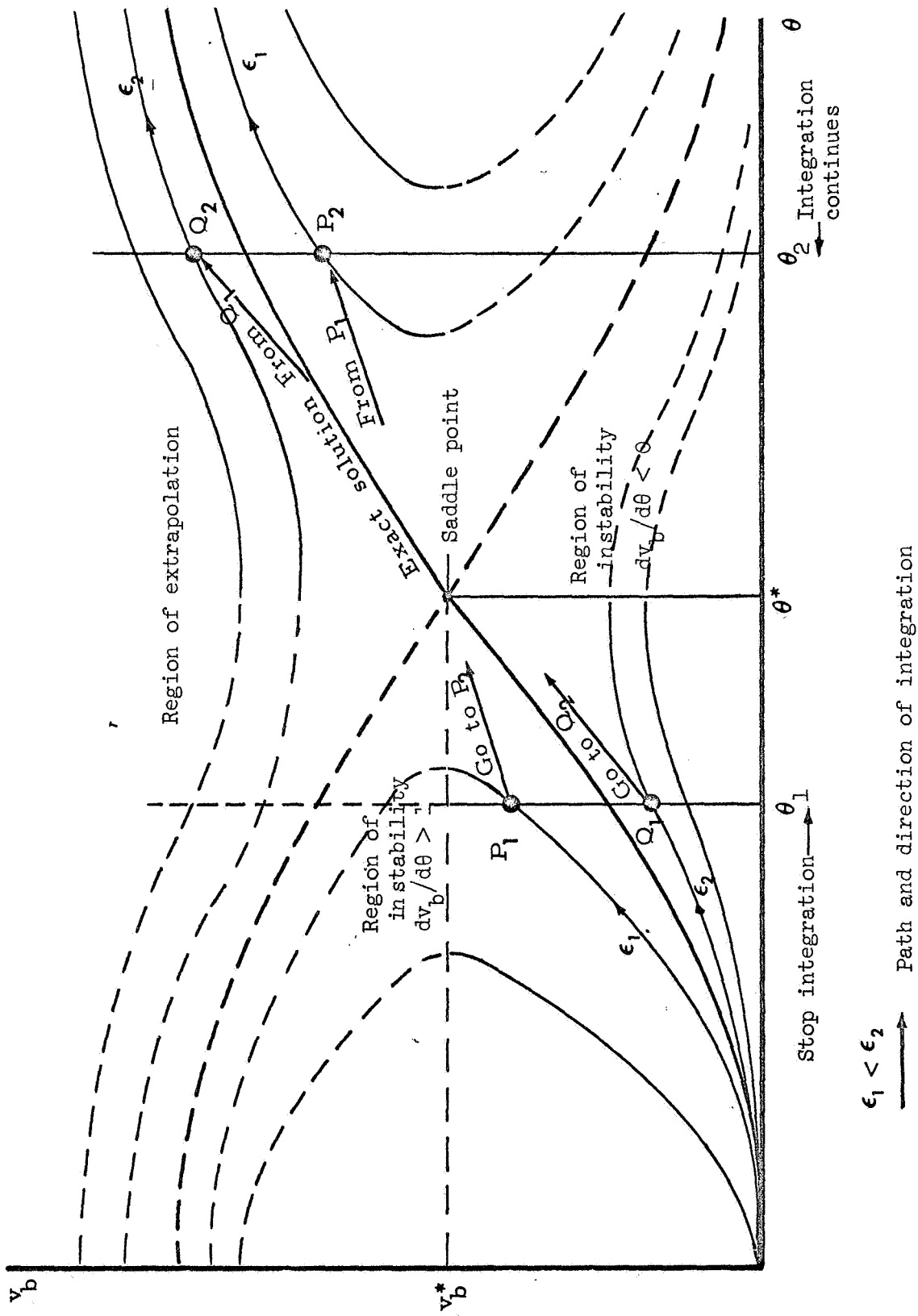


FIG. 5.1 INTEGRAL CURVES FOR v_b AND SADDLE POINT

Once the detachment distance is known with sufficient accuracy, the problem of finding the location of the sonic point on the body remains to be solved. To do that, it is necessary to stop the integration a few steps before the sonic point and with the value of the derivative found for the last point one can extrapolate until the point for which the velocity v_p equals v^* , is reached. Should one desire to carry the integration beyond the sonic point, a further extrapolation has to be carried out as it is indicated in Figure 5.1, where the jump in the extrapolation occurs from the point P_1 to the P_2 or from Q_1 to the Q_2 depending on the curve along which the integration has been carried.

5.8 Calculations in the Shock Layer

The calculations in the shock layer were carried out in the manner described in paragraph 5.5. The sonic line was found as the locus of the points in which the Mach number is one. If the value of the azimuth of all points on the sonic line is less than the one that corresponds to the sonic point on the body, it is not necessary to pass through the saddle point, and the solution simplifies to some extent because the calculations beyond the saddle point can be obtained by the method of the characteristics since the ray that passes through the sonic point is totally beyond the transonic region, i.e., it is located downstream of the limiting characteristic as was already discussed in Section 2.

6. RESULTS

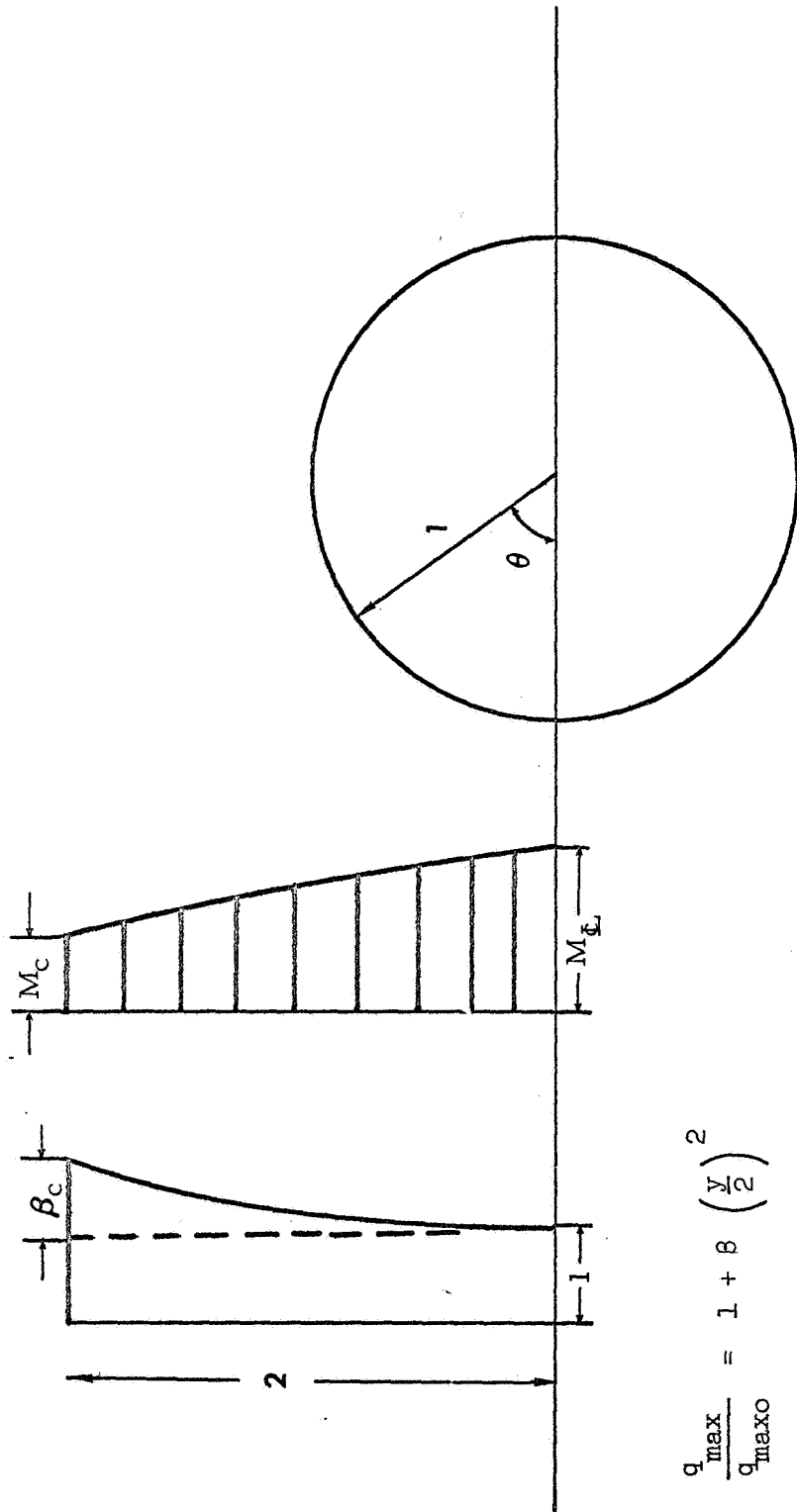
6.1 Description of the Different Cases under Investigation

Figure 6.1 describes the different parameters that define each of our cases. As is indicated in the Figure, parabolic distributions of the q_{\max} and Mach number have been adopted. M_c represents the Mach number at a distance $2 R$ from the axis and M_{cl} represents the Mach number at the center line. The parameter β_c represents the fractional excess in the maximum velocity at $y = 2 R$ over the value of q_{\max} . The different cases considered in these calculations correspond then to those defined in Table I.

Case I corresponds to the uniform flight of the sphere for Mach number 4.0. Case II has a uniform stagnation temperature but variable Mach number. Case III is under uniform Mach number but variable stagnation temperature. And finally Case IV is a superposition of Cases II and III.

6.2 Results

Computations for the cases above defined were carried out in a digital computer IBM 360/75 and the program was written in FORTRAN IV. The average time to compute ϵ_{iex} with 6 decimal digits was variable for each case, but it was of the order of 6 minutes when it was done manually, that is, observing the output for each run and deciding on a new value for ϵ_i . If the computation had been done automatically the time would have increased to ten minutes.



$$\frac{q_{\max}}{q_{\max 0}} = 1 + \beta \left(\frac{y}{2} \right)^2$$

$$M(y) = M_{\bar{c}_1} - (M_{\bar{c}_1} - M_c) \left(\frac{y}{2} \right)^2$$

FIG. 6.1 DEFINITION OF INPUT PARAMETERS

TABLE I
INPUT PARAMETERS

CASE NUMBER	1	2	3	4
β_c	0.0	0.0	-0.5	-0.5
M_c	4.0	4.0	4.0	4.0
M_c	4.0	2.0	4.0	2.0

TABLE II
NUMERICAL RESULTS

CASE NUMBER	1	2	3	4
ϵ_i	0.175	.200	.169	.187
θ_b^*	.73	.93	.69	.89
θ_{sh}^*	.57	.55	.54	.52

The significant numerical data for each case are shown in Table II, where θ_b^* is the azimuth of the sonic point at the body, θ_{sh}^* is the azimuth of the sonic point behind the shock. ϵ_{iex} is the stand-off distance of the shock at the center line.

Figure 6.2 shows the shock shape and sonic line for Case I according to the present method (dashed lines). The numerical results of the three strip solution of Belotserkovskii [6.1] are given for comparison (see full lines). The apparent peculiarity in the computed sonic point near the body is discussed in the next section. In Figure 6.3 the difference between the Belotserkovskii solution and the present solution is amplified. It should be noted that the origin of the vertical scale is at 1.5. Figure 6.4 illustrates the variation of pressure across the shock layer; the differences have been amplified again for purposes of comparison. One can say that the maximum differences in the shock stand-off distance is of the order of 0.5% and that the pressure differs less than 5% across the shock layer.

Figure 6.5 compares the shock and sonic lines for cases I and II. The same technique used for Case I has been used for Case II. Figure 6.6 shows the variation of pressure across the shock layer for Cases I and II. It should be noticed that for Case II the pressure behind the shock seems to remain constant along the azimuthal direction.

In Figure 6.7 the pressure variation has been plotted along the body for Case I and in Figure 6.8 the difference for Cases II, III, and IV is shown; the maximum variations correspond to Case II and it is of the order of 25%.

————— Belotserkovskii's three strips solution
 - - - - - Actual one strip solution
 ○○○○○○ Sonic points

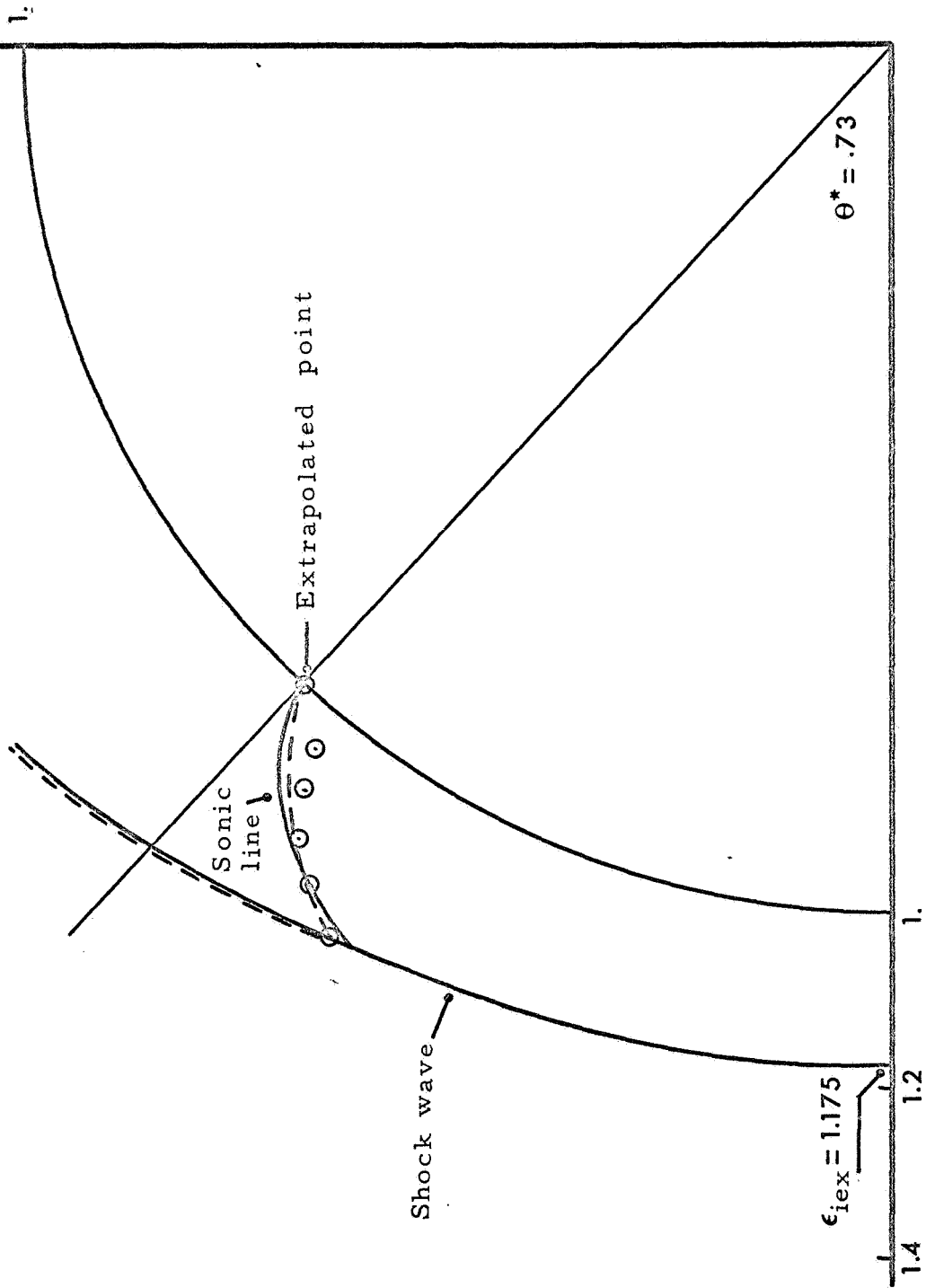


FIG. 6.2 FLOW PATTERN FOR THE UNIFORM FLIGHT OF A SPHERE

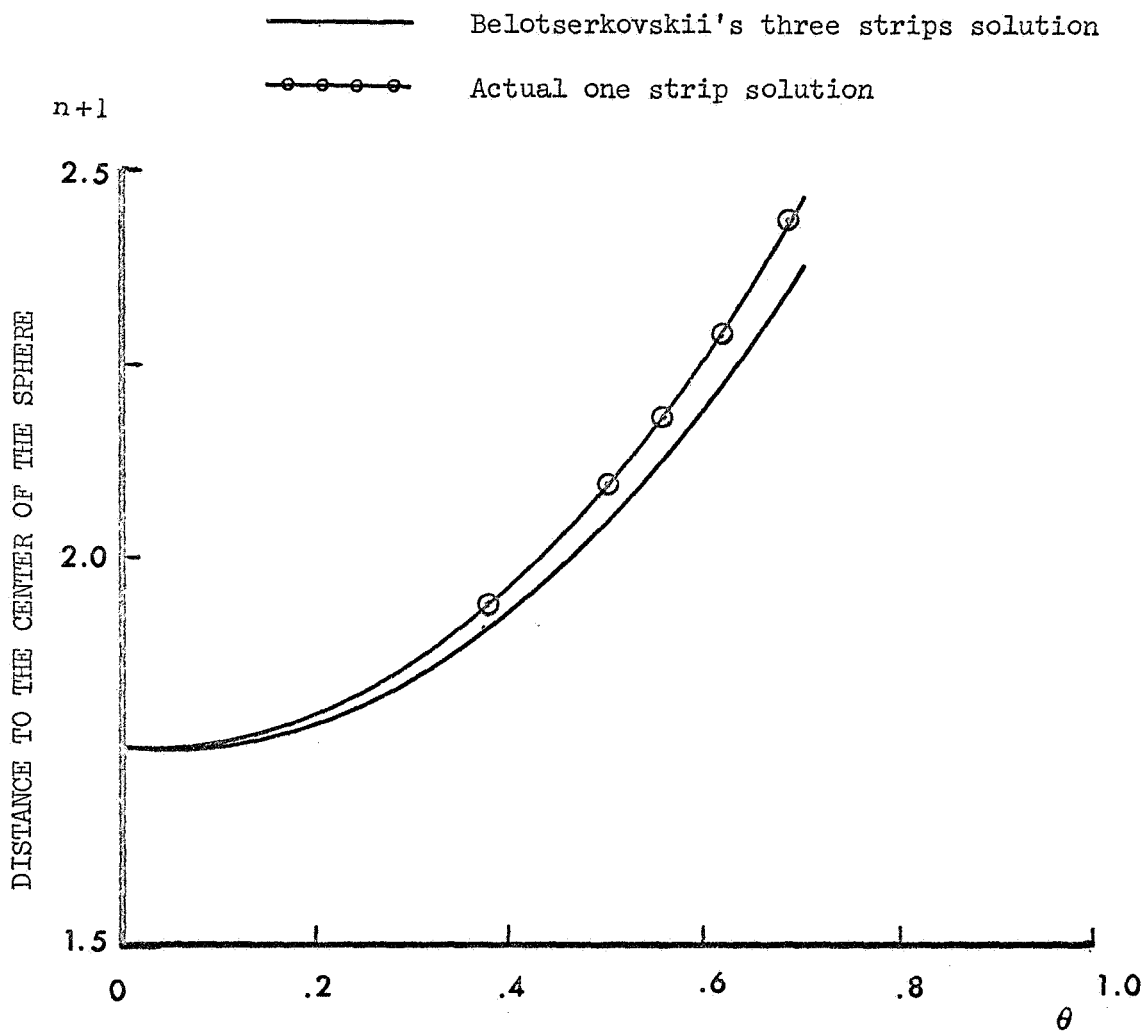


FIG. 6.3 SHOCK SHAPE SOLUTION FOR CASE I
 BY THE ACTUAL METHOD AND BELOTSEKOVSKII'S

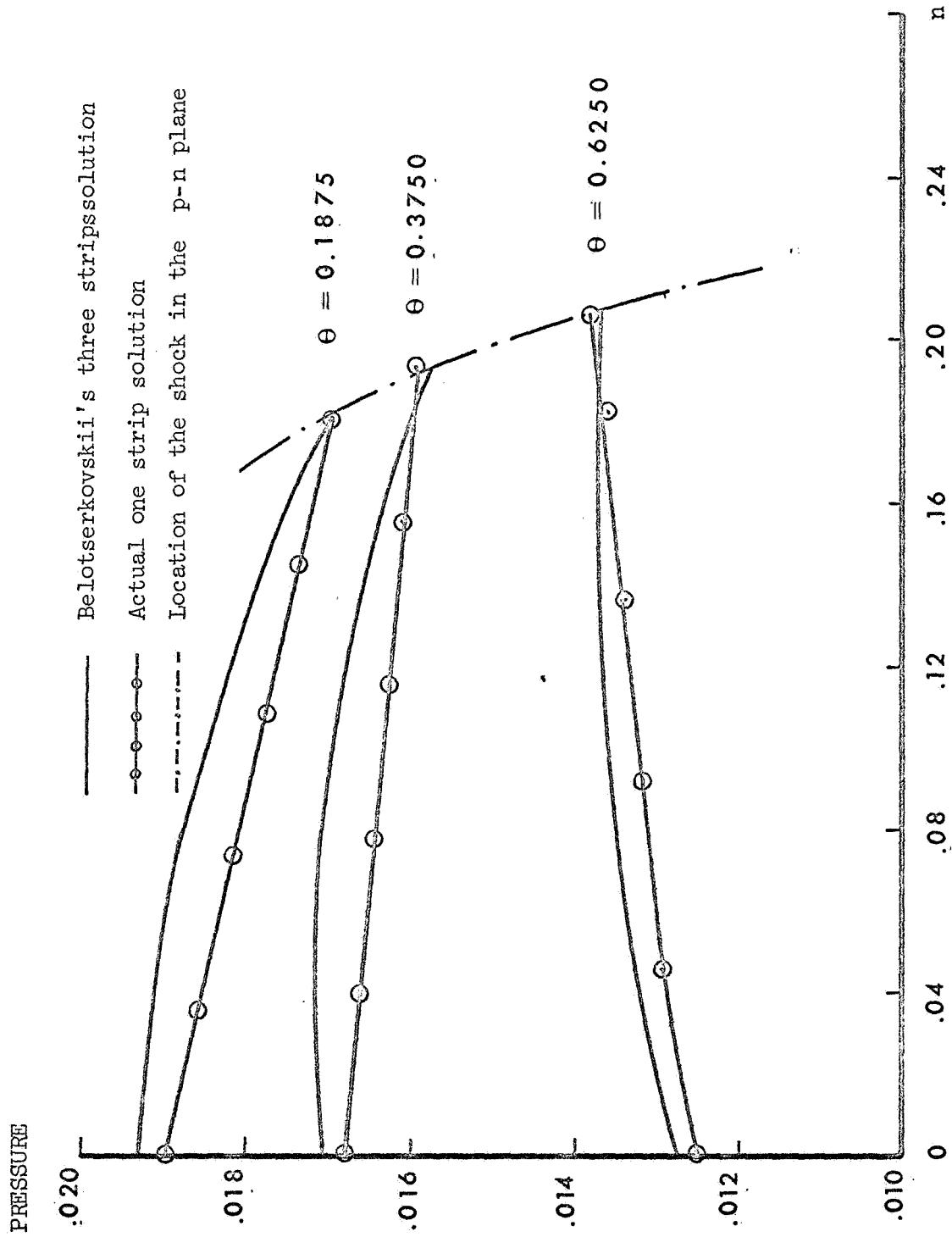


FIG. 6.4 DISTRIBUTION OF PRESSURE VERSUS n FOR VARIOUS θ

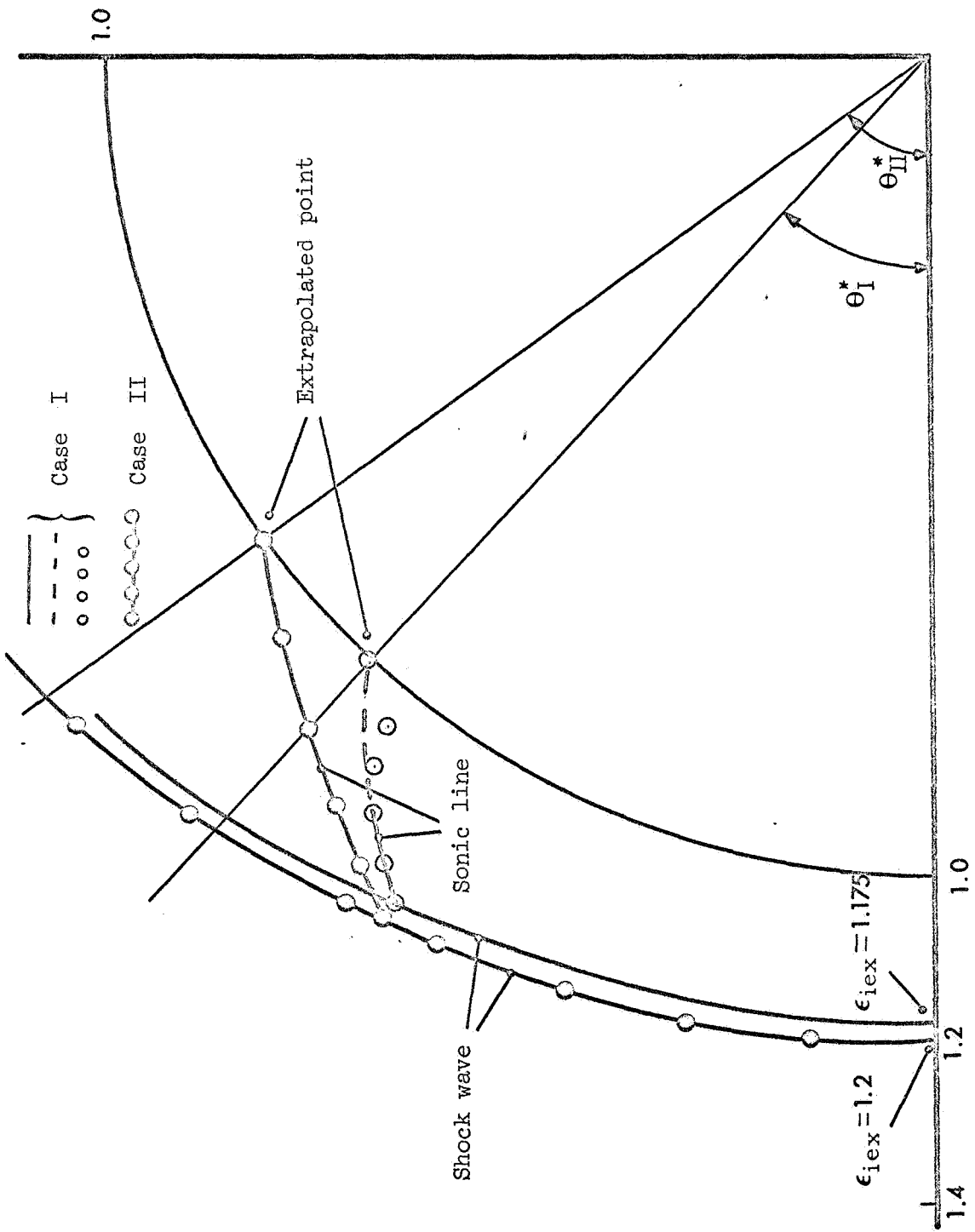


FIG. 6.5 FLOW PATTERN FOR CASES I AND II

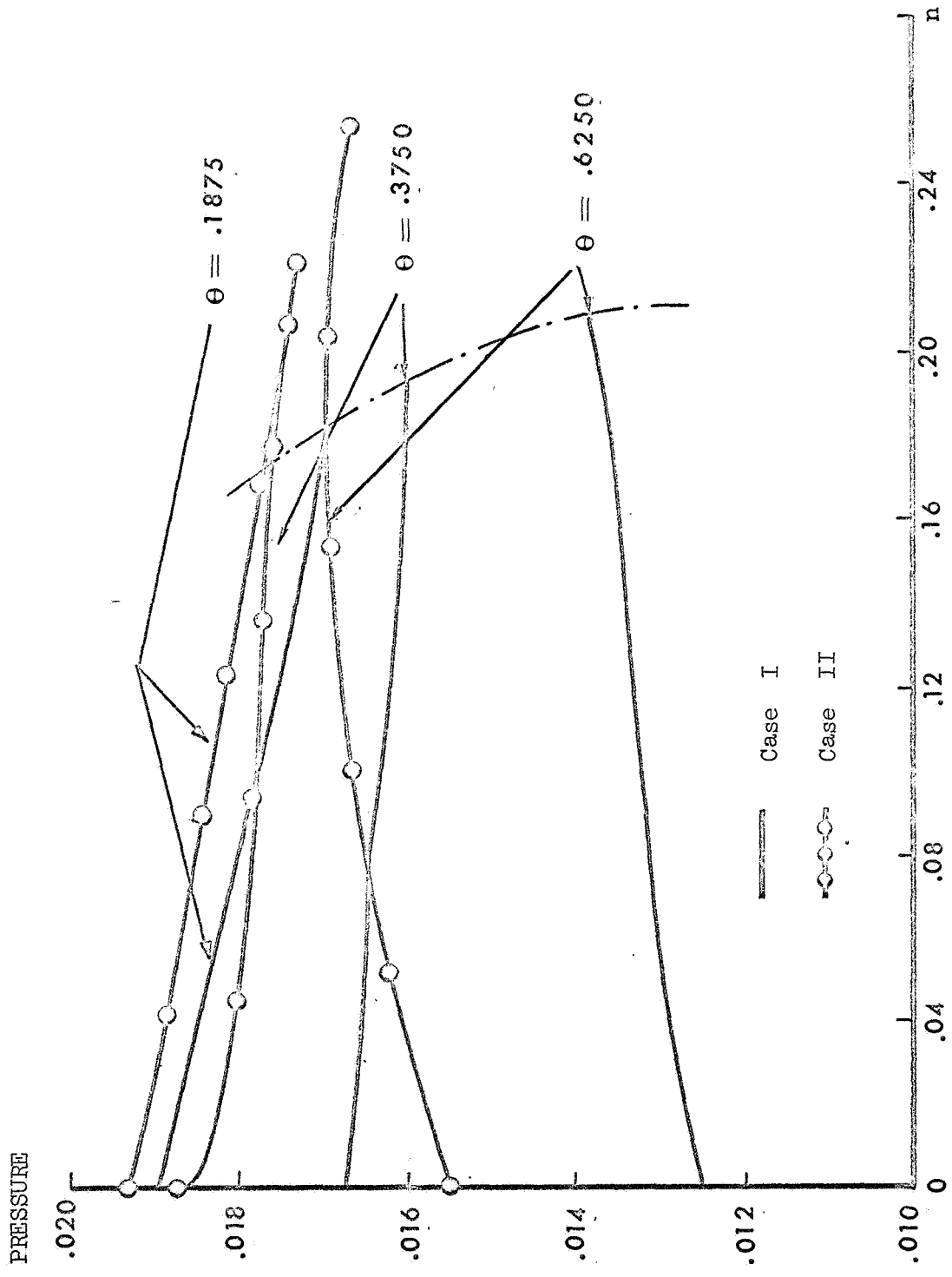


FIG. 6.6 DISTRIBUTION OF PRESSURE ALONG n FOR VARIOUS θ FOR CASES I AND II

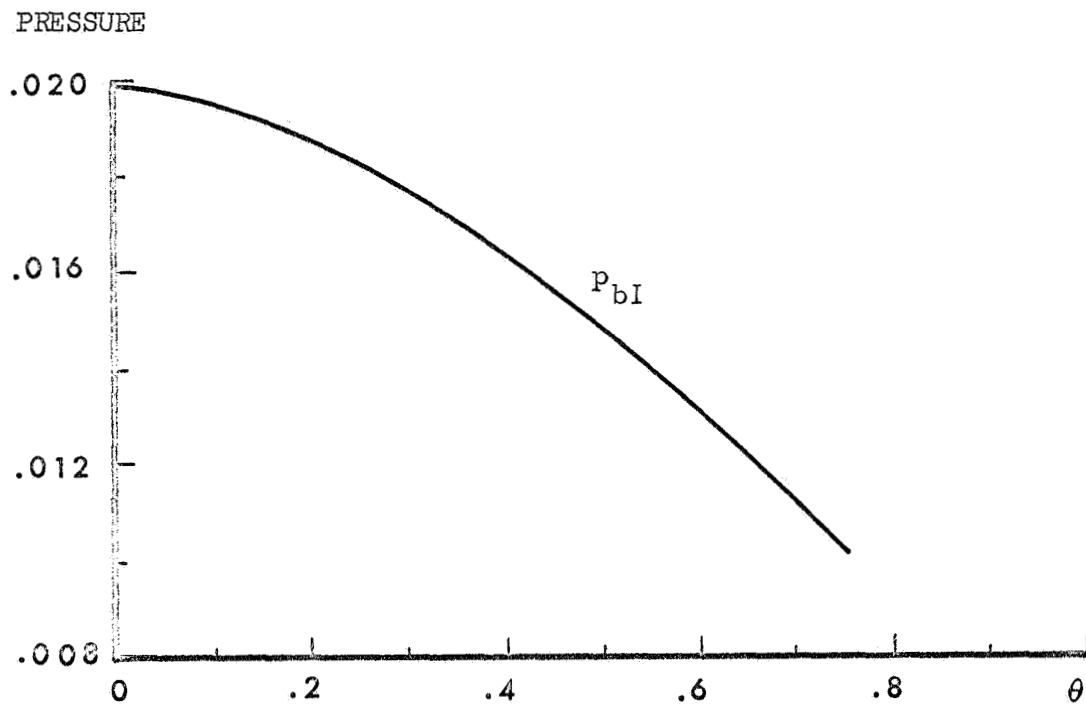


FIG. 6.7 PRESSURE DISTRIBUTION ON THE BODY FOR CASE I

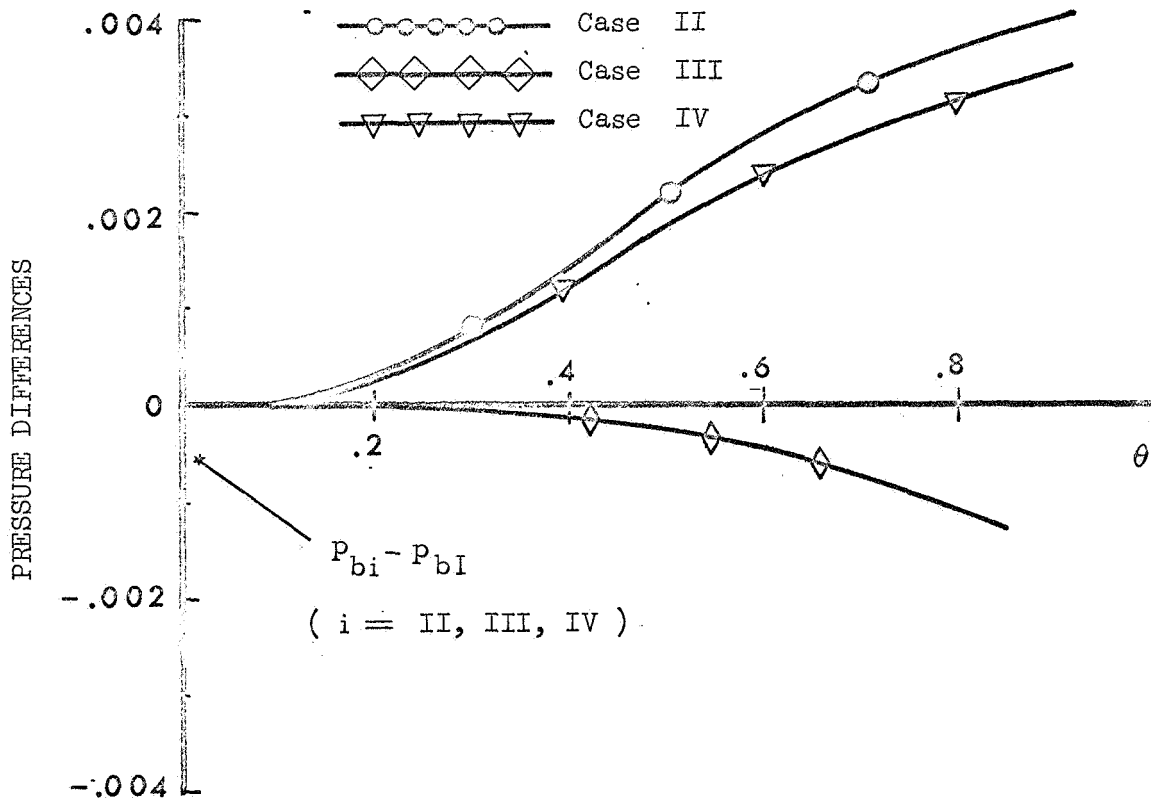


FIG. 6.8 PRESSURE DIFFERENCES BETWEEN CASES II, III, IV AND I

In Figure 6.9 the temperature variation along the body is shown, and in Figure 6.10 the differences with Cases II, III, IV are shown. The largest difference occurs again for Case II and it is of the order of 7%.

Figure 6.11 shows, with the vertical scale amplified, the shock waves for the different cases. The maximum change occurs for Case II and it is about 10% at the center line.

Figures 6.12, 6.13, 6.14, 6.15, and 6.16 correspond to the distributions of velocity at the body along the azimuthal direction and their differences. The maximum difference is for Case II and is of the order of 25%.

For further details on the results the reader is referred to the corresponding figures. Special care should be taken when considering vertical scales with regard to the order of magnitude and the shifting of the origin.

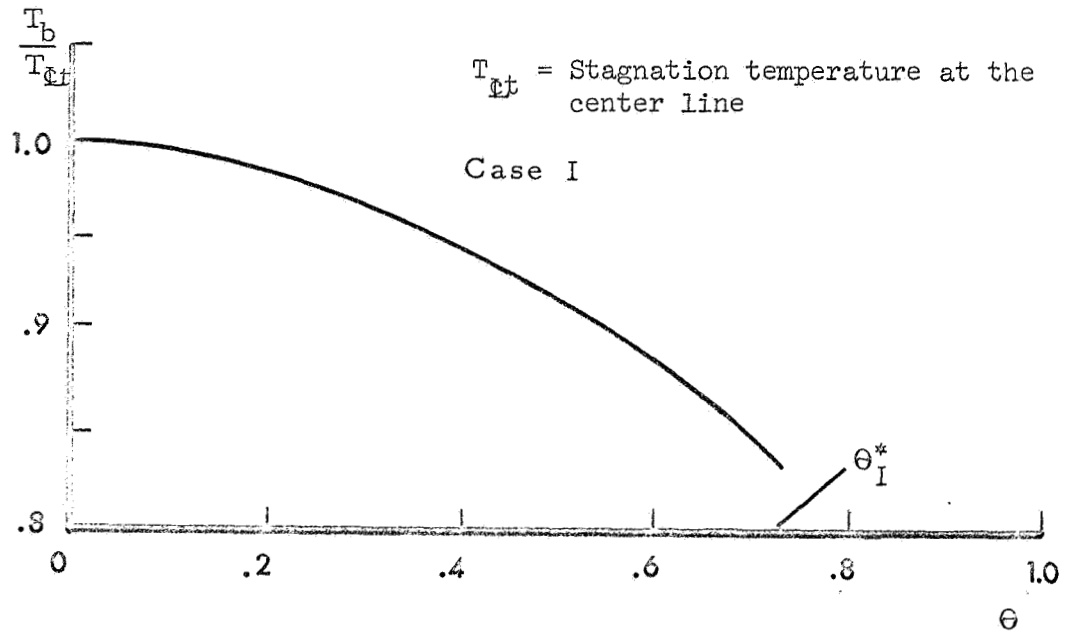


FIG. 6.9 TEMPERATURE DISTRIBUTION ALONG THE BODY

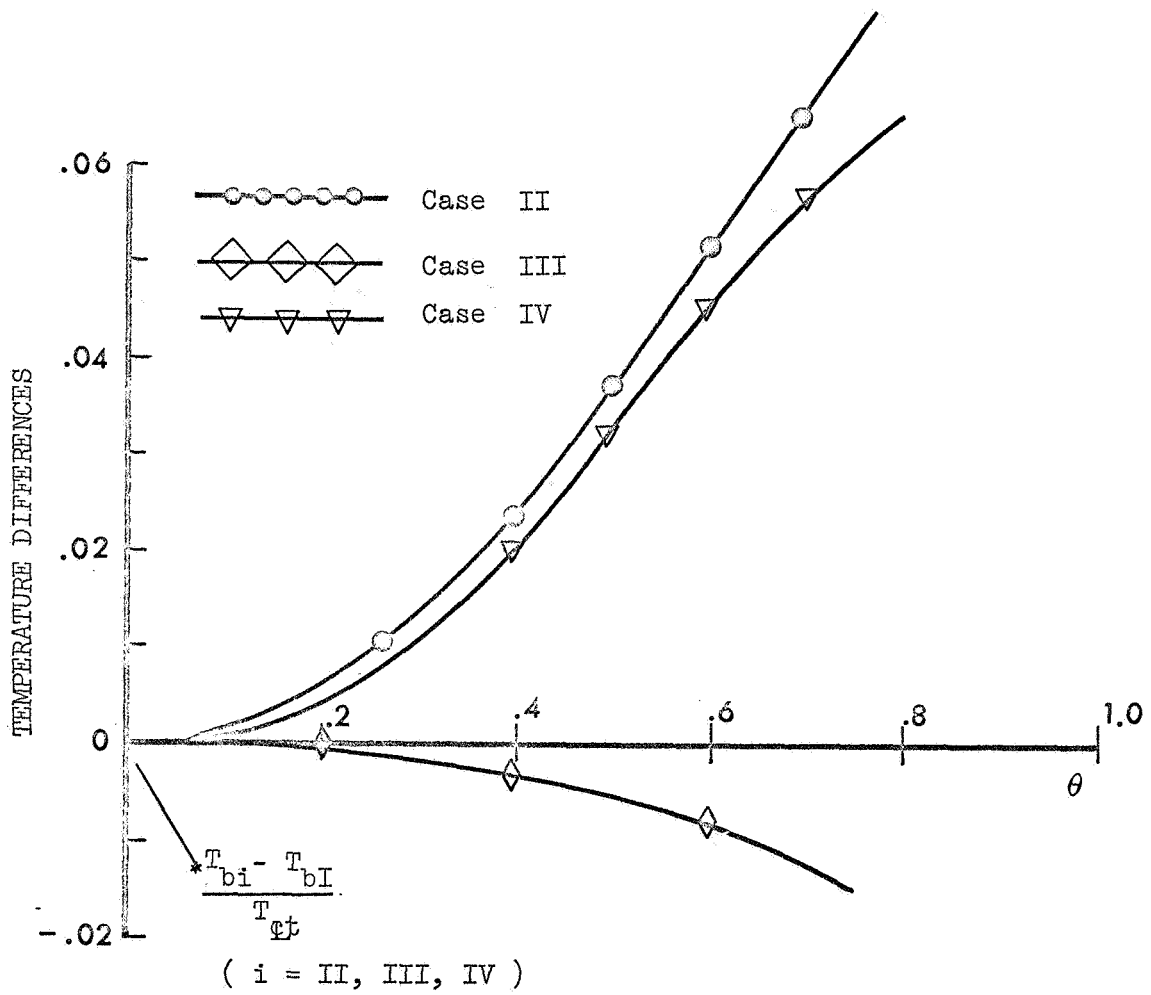


FIG. 6.10 STATIC TEMPERATURE DIFFERENCE FOR THE DIFFERENT CASES

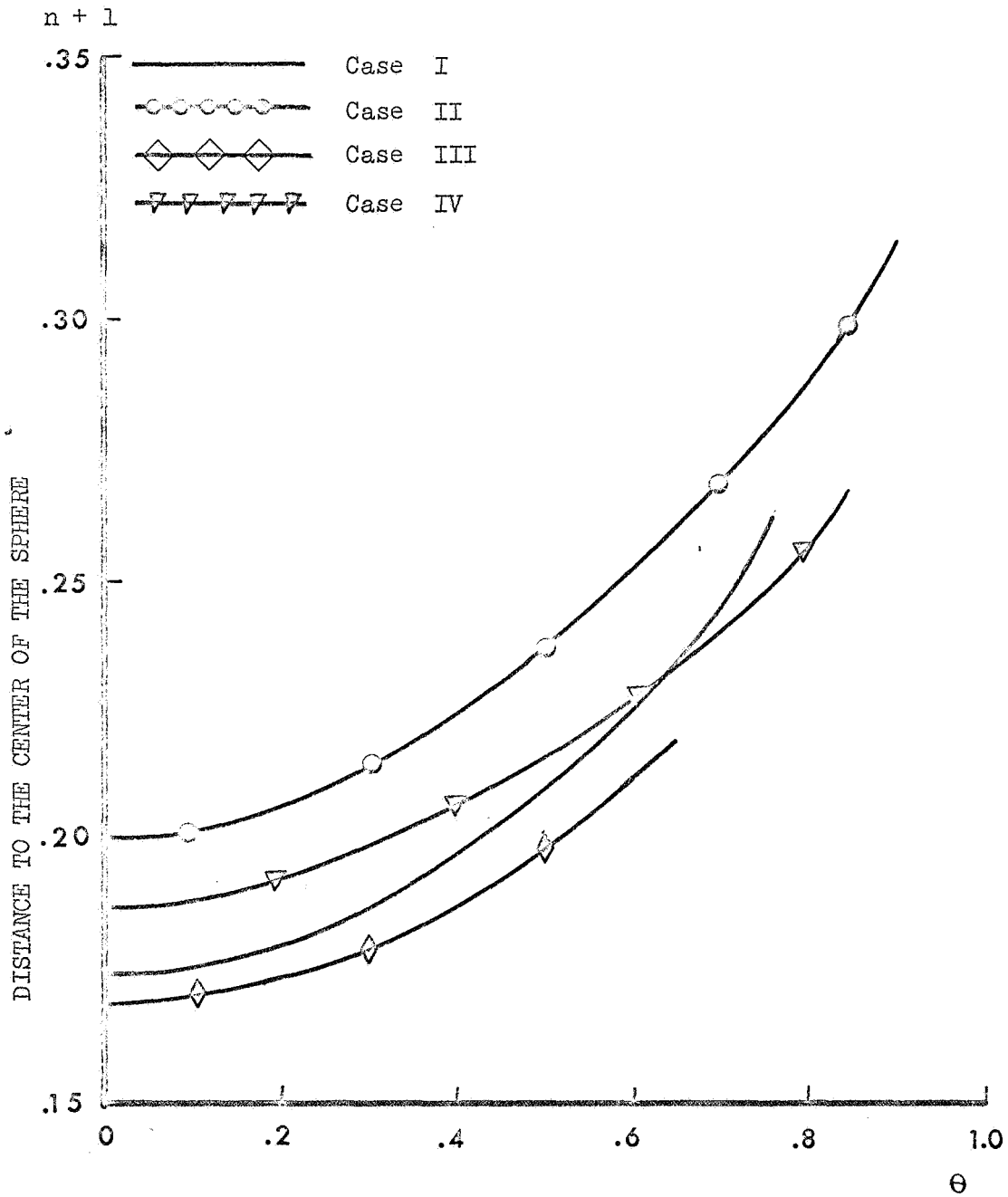


FIG. 6.11 SHOCK WAVE SHAPES FOR THE DIFFERENT CASES

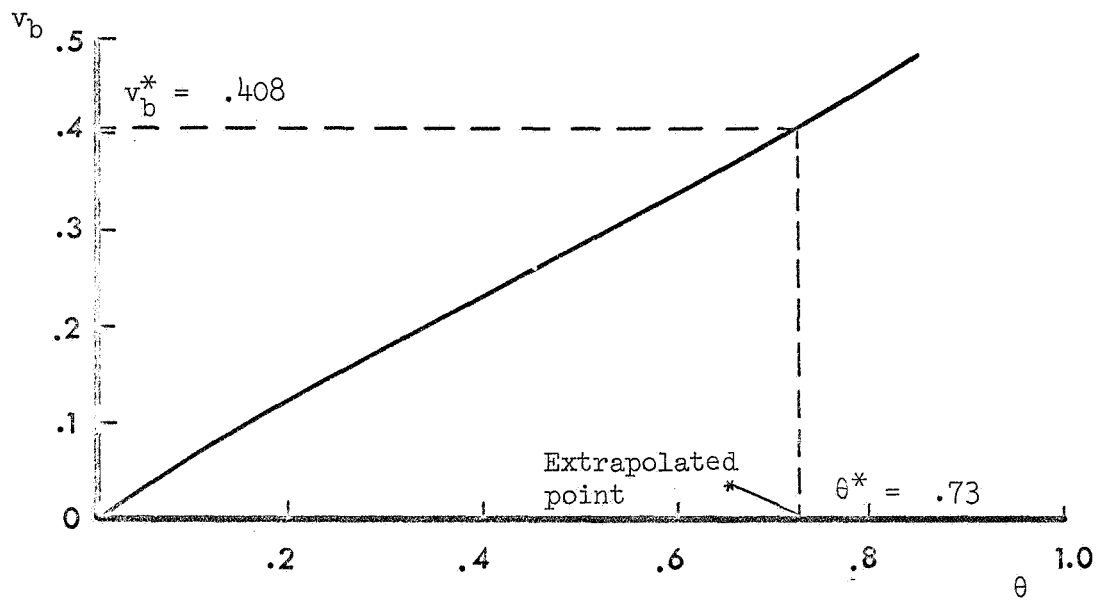


FIG. 6.12 VELOCITY DISTRIBUTION ON THE BODY FOR CASE I

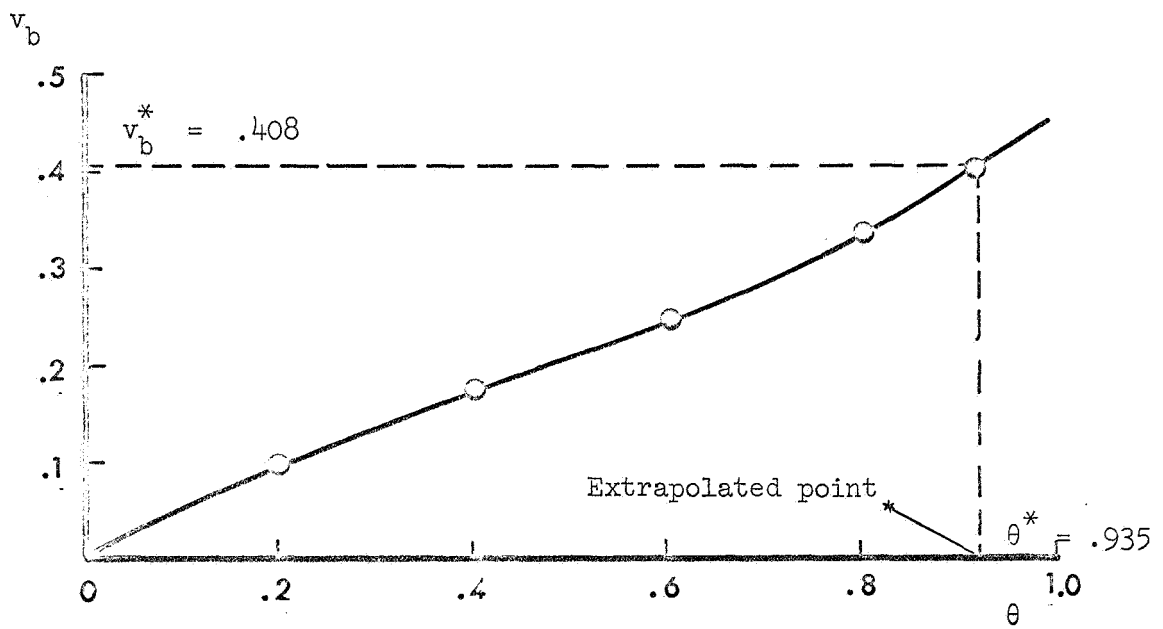


FIG. 6.13 VELOCITY DISTRIBUTION ON THE BODY FOR CASE II

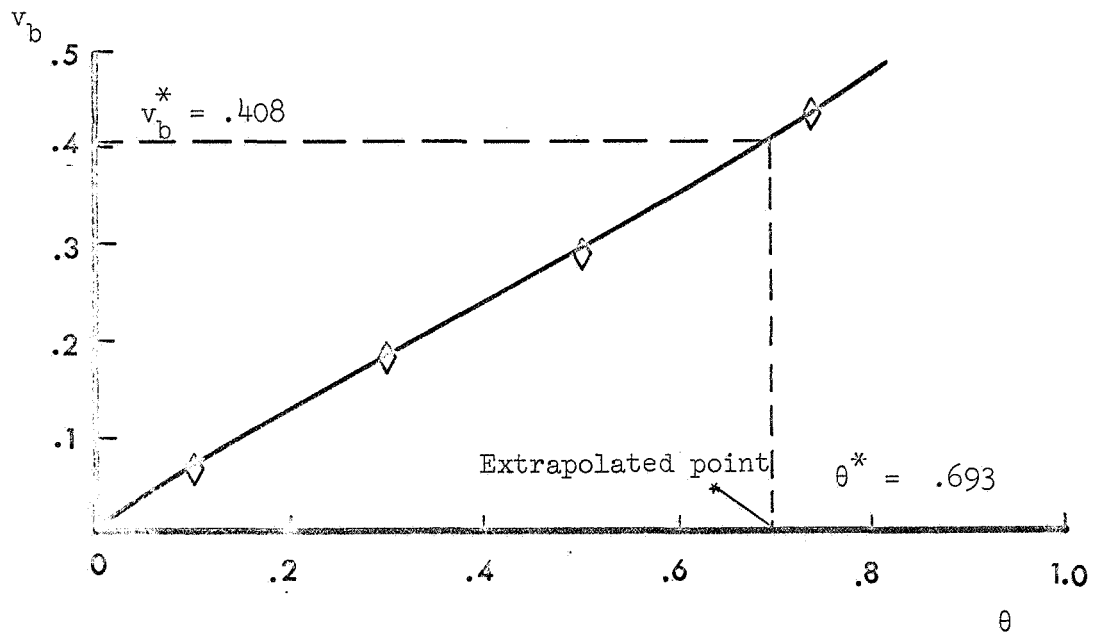


FIG. 6.14 VELOCITY DISTRIBUTION ON THE BODY FOR CASE III

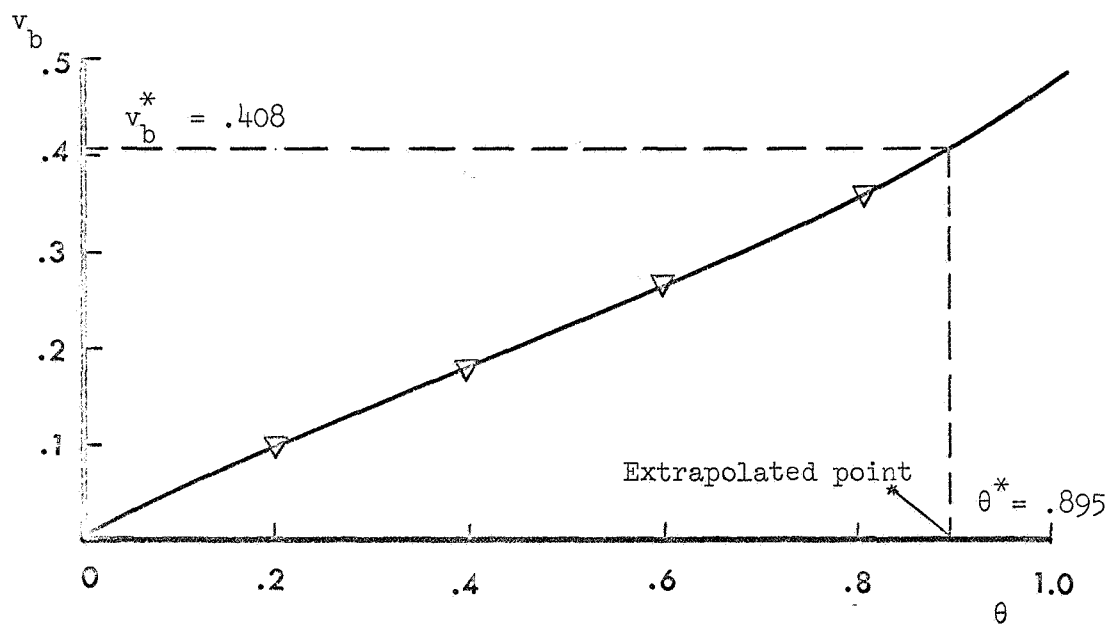


FIG. 6.15 VELOCITY DISTRIBUTION ON THE BODY FOR CASE IV

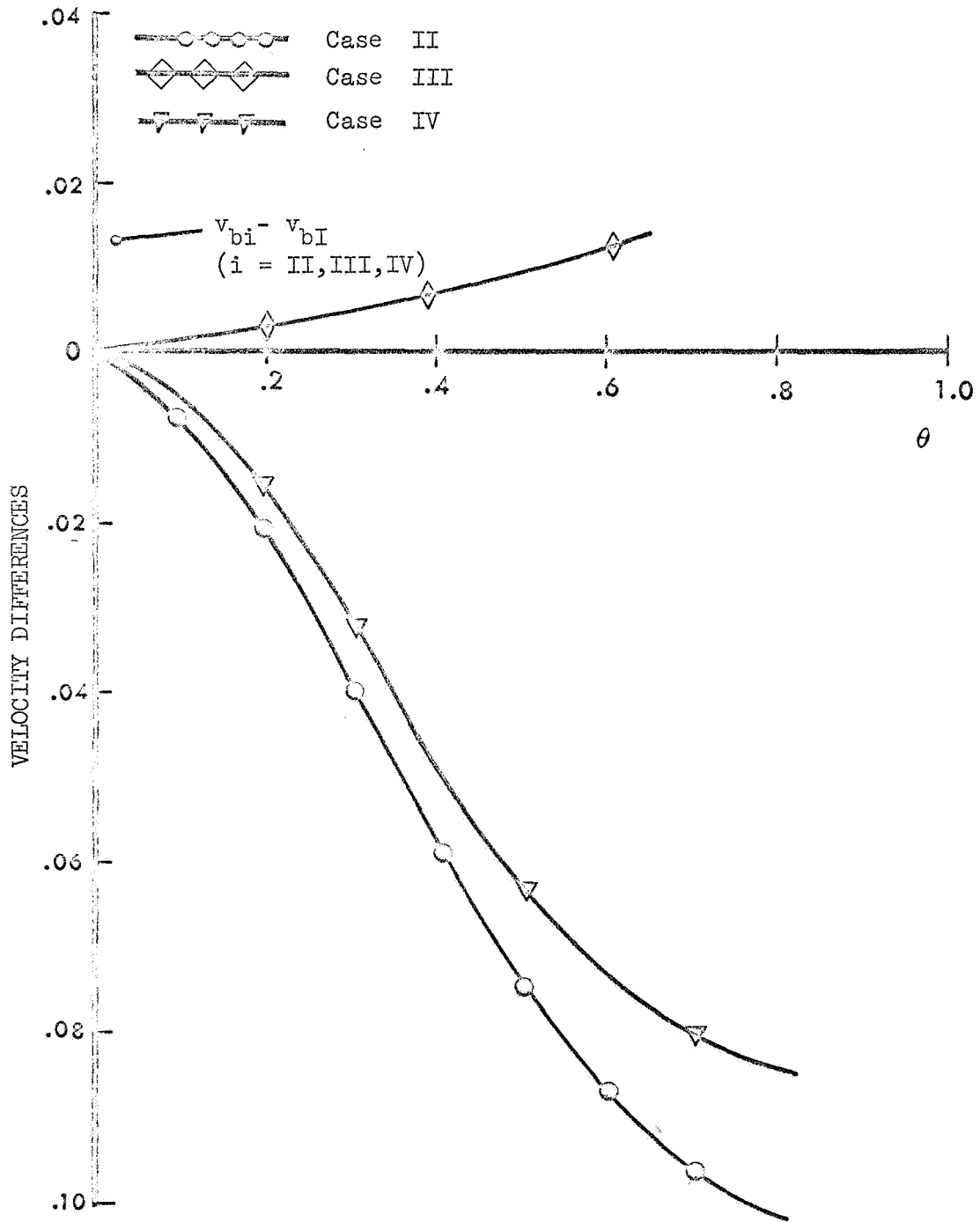


FIG. 6.16 VELOCITY DISTRIBUTION DIFFERENCES FOR CASES II, III, IV, AND I

7. DISCUSSION OF RESULTS

As one can see from Figure 6.2 and 6.3, the one strip method as developed in this study approximates the shape of the shock wave very closely; the approximation becomes worse for values of θ larger than that corresponding to the sonic point on the shock. The sonic line, on the other hand, is approximated only qualitatively. The sonic point on the body, which has been calculated by extrapolation of the integral curve, $v_b - \theta$, for one of the best estimates of ϵ_{iex} as already mentioned in earlier sections, coincides with that given in the three strip solutions. Figure 6.11 was utilized for this purpose and if only three significant decimal digits for θ^* are desired, there is no significant difference between the upper or lower bounds of ϵ_{iex} which are used in the extrapolation. The other sonic points encircled in Figure 6.2 were calculated by carrying calculations in the shock layer, in the manner mentioned in Section 5, using the computed results of a case representing the best of the bounds on ϵ_{iex} . As one can see, the internal sonic points closer to the wall do not converge to the extrapolated sonic point on the body, and therefore the sonic points close to the wall are not expected to be reliable. The reason for this disparity could be the sensitivity of the solution in a neighbourhood of the saddle point to the accuracy of the approximated stand-off distance.

In Figure 6.4 one can see additional effects of the first approximation as compared with the more exact three strips solution. The reason for the near linear pressure distribution for lower values of

the azimuth for 1-strip method case is due to the fact that in the region close to the stagnation streamline, the density remains nearly constant and the velocity component along the azimuthal direction is very small; but the one strip method results in the linear approximation of the quantity Y defined in Equation (3.17), which for the case of the sphere becomes

$$Y = (2p + \rho v^2) y \approx 2p y \quad (7.1)$$

Taking into account that y remains almost constant across the shock layer if $y \ll 1$, one obtains approximately a linear variation of p as shown by the numerical results. For larger values of the azimuth, v is no longer small, y varies significantly across the shock layer and the density cannot be assumed constant anymore, and therefore the pressure distribution is expected to deviate from the linear behaviour.

Figure 6.5 shows the same results as in Figure 6.2, but for Cases I and II. The most remarkable feature is the large extension of the subsonic region along the body for Case II as compared with Case I. The shock wave moves outward, and only the sonic point on the shock remains approximately in the same area (although this fact does not seem to have any physical significance). It should be noted that a remarkable improvement in the solution for the sonic line behaviour next to the body as compared with Case I is evident. There is no explanation for such a feature at the present time.

An examination of Figure 6.5 shows that the pressure across the shock layer for Case II behaves qualitatively in the same manner as

that for Case I. One can observe a rise in pressure on the body, and a more exaggerated rise behind the shock. As one can see, the pressure behind the shock remains more or less constant for the three values of θ displayed. This result is caused by the deformation of the shock wave that becomes less steep as compared with Case I, as can be seen in Figure 6.11. Also, in this Figure are displayed the shock shapes for Cases III and IV. It is seen that the shocks are always flatter than for Case I, and it seems that this effect is most significant for Case IV.

Figures 6.7 and 6.8 show the pressure on the body for case I and the differences with the other cases. These curves show an increase in body pressure as one approaches the sonic point of Case I, even though the mean Mach number is smaller for Case II. This is due to the fact that, for this particular case, the dynamic pressure in the free stream, ρq_{∞}^2 , increases in the radial direction. In the Newtonian approximation the body normal, free stream dynamic pressure is directly related to the body pressure and thus the above result is understandable. This increase in pressure is most marked close to the sonic point, and, therefore, the increase in the drag coefficient will not be significant since both the pressure and the horizontal component of the pressure in that region are small as compared with that in the stagnation region. For Case III, a variation in stagnation enthalpy, the effect is opposite although much smaller. For Case IV, a combined variation case, one can see that the radial heating and Mach number variations have opposite effects with the Mach number variation dominating.

Figures 6.9 and 6.10 show the temperature variation on the body for the different cases in an analogous manner as was done with the pressure. It is seen that the body temperature profile for Case II is larger than for Case I which is larger than for Case III. This result is expected in that the stagnation enthalpy along the body is the same for all cases and therefore the profile is dictated by the location of the sonic point. Once again, Case IV shows that the effects just described are opposite when acting simultaneously, but again the Mach number variation dominates.

Finally, Figures 6.11, 6.12, 6.13, 6.15, 6.16 show the velocity variation on the body for each case and their final comparison. These figures were used for computing the extrapolated sonic point, and since in all the cases the θ of this point was larger than that one of the internal sonic points, no integration beyond the sonic point on the body was necessary as was discussed in the last section.

The shock layer properties for Cases III and IV were not computed and nothing can be said about their behaviour across the shock layer and along the sonic line.

8. RECOMMENDATIONS AND CONCLUSIONS

The method described can be generalized to include stagnation pressure variations in the free stream with no complex modifications. Should one include asymmetric non-uniformities the problem becomes quite involved and it is of a nature similar to the blunt body under an angle of attack. If keeping the symmetry in the non-uniformities one desires to introduce cross flow (i.e., the velocity in the free stream has a radial component) it can be introduced with no substantial modifications if one knows the analytical law for the radial component. Finally, if the Mach number decay along the radial direction goes to values of the Mach number less than one, the problem cannot be solved under the present analysis and an investigation of a new numerical technique is required.

In conclusion one can say that for the cases studied

- a) The non-uniformities affect the shock wave to some extent.
- b) The shock wave becomes less steep than for the uniform case.
- c) The most sensitive parameter to the non-uniformities is the location of the sonic point on the body.
- d) This change in location changes the drag coefficient by an amount that is much smaller than the percentage of change of the non-uniformities.
- e) Since the entropy layer in the supersonic region of the flow around the body depends on the changes in curvature of the shock, it seems that this layer will suffer the major effects of the non-

uniformities. Since the shock for these cases has continuously less curvature, the extension of the entropy layer will be enlarged. Note that the free stream was already a non-isentropic layer for the non-uniform cases.

REFERENCES

SECTION 1

- 1.1. W.D. Hayes and R.F. Probststein, Hypersonic Flow Theory, Vol. 1, pp 391, Academic Press, New York, 1966.
- 1.2. H. Lomax and M. Inouye, "Numerical analysis of flow properties about blunt bodies moving at supersonic speeds in an equilibrium gas," NASA TR R-204, 1964.
- 1.3. R. J. Swigart, "Real gas hypersonic blunt body flows," AIAA J, 1, 1034-1042 pp, 1963.
- 1.4. R. Vaglio-Laurin, "On the PLK method and the supersonic blunt body problem," IAS Paper 61-22, January 1961.
- 1.5. J.G. Hall, A.Q. Eschenroeder, P.V. Marrone, "Inviscid hypersonic air flows with coupled chemical reactions," J. Aerospace Sci., 29, p 1038, 1962.
- 1.6. W. Hayes, R. Probststein, Hypersonic Flow Theory, Academic Press Inc., New York, 1959.
- 1.7. S.H. Maslen, W.E. Moeckel, "Inviscid hypersonic flow past blunt bodies," J. Aerospace Sci., 24, pp 683-693, 1957.
- 1.8. F.Y. Gravalos, I.H. Edelfelt, H.W. Emmons, "The supersonic flow about a blunt body of revolution for gases at chemical equilibrium," Proceedings of the 9th Congress of the International Astronautical Federation, Amsterdam, 1958 (Springer-Verlag, Vienna, 1959).
- 1.9. O.M. Belotserkovskii, P.I. Chuskin, "The numerical solution of problems in gas dynamics," Basic Developments in Fluid Dynamics, edited by M. Holt, Academic Press Inc., New York, pp 1-126, 1965.
- 1.10. I.O. Bohachevsky, E.L. Rubin, "A direct method of computation of non-equilibrium flows with detached shock waves," Pt. I, AIAA Preprint 65-24, January 1965.
- 1.11. I.O. Bohachevsky, R.E. Mates, "A direct method of computation of non-equilibrium flows with detached shock waves," Pt. II, AIAA Preprint 65-24, January 1965.
- 1.12. G. Moretti and M. Abett, "A Time-Dependent Computational Method for Blunt Body Flows," AIAA J, 4, no. 12, December 1966.

- 1.13. B.S. Masson, "Two Dimensional Flow Field Calculations by the Godunov Method," Aeronutronic Report No. V-4137, June 1967.
- 1.14. B. Edney, "Anomalous Heat Transfer and Pressure Distributions on Blunt Bodies at Hypersonic Speeds in the Presence of an Impinging Shock," The Aeronautical Research Institute of Sweden, Report 115, 1968.
- 1.15. O.M. Belotserkovskii, "Supersonic symmetrical flow of perfect and real gases about blunt bodies," J. Computing Math. and Math. Phys. (Russian). 2, pp 1062-1085, 1962.

SECTION 2

- 2.1. W.D. Hayes and R.F. Probstein, Hypersonic Flow Theory, Vol. 1., pp 391, Academic Press, New York, 1966.
- 2.2. P.D. Lax and B. Wendroff, "Difference Schemes with High Order of Accuracy for Solving Hyperbolic Equations," NYU 9759, AEC Computing and Applied Mathematics Center, Courant Institute of Mathematical Sciences, New York University, 1962.
- 2.3. P.D. Lax, "Weak Solutions of Non-Linear Hyperbolic Equations and their Numerical Computation," Comm. on Pure and Appl. Math., 7, No. 1, pp 159-193, 1954.
- 2.4. S.K. Godunov, A.V. Zabrodin, and G.P. Prokopov, "The Difference Schemes for Two-Dimensional Unsteady Problems in Gas Dynamics and the Calculation of Flows with a Detached Shock Wave," Translation from the Journal of Computing Mathematics and Mathematical Physics, Academy of Sciences, USSR, 1, No. 6, November-December 1961, translated by I. Behachevsky.
- 2.5. S.K. Godunov, "Finite Difference Method for Numerical Computation of Discontinuous Solutions of the Equations of Fluid Dynamics," Mat. Sbornik, 47, No. 3, p 271, 1959, translated by I. Behachevsky.
- 2.6. B.S. Masson, "Two-Dimensional Flow Field Calculations by the Godunov Method," Aeronutronic Report No. V-4137, June 1967.
- 2.7. D.W. Eastman and J.P. Bonema, "Flow Field of a Highly Underexpanded Jet Impinging on a Surface," AIAAJ, 4, No. 7, p 1302, July 1966.
- 2.8. H. Yashihara, "Rocket Exhaust Impingement on a Ground Surface," Journal of Fluid Mech., 15, p 65, 1962.

SECTION 4

- 4.1. H.E. Bethel, "On the Convergence and Exactness of Solutions of the Laminar Boundary-Layer Equations Using the N-Parameter Integral Formulation of Galerkin-Kantorovich-Dorodnitsyn," Aero-Space Research Laboratories, June 1966, Ph.D. Thesis, Purdue U.
- 4.2. A.A. Dorodnitsyn, "On a Method of Numerical Solution of Some Non-Linear Problems of Aero-Hydrodynamics," Proc. 9th Internatl. Congr. Appl. Mech., Vol. I, p 485, Univ. of Brussels, Brussels, 1957.
- 4.3. O.M. Belotserkovskii, and V.K. Chuskin, "The Numerical Solution of Problems in Gas Dynamics," Basic Developments in Fluid Dynamics, Vol. I (M. Holt, ed.), pp 1-126, Academic Press, New York, 1965.
- 4.4. A.A. Dorodnitsyn, "A Contribution to the Solution of Mixed Problems of Transonic Aerodynamics," Advances in Aeronautical Sciences, Vol. 2 (Th. von Karman, Chmn. ed. comm.), pp 832-943, Pergamon, New York, 1959.
- 4.5. A.A. Dorodnitsyn, "Numerical Methods in Gas Dynamics," Arch. Mech. Stos., 12, pp 13-27, 1960.
- 4.6. A.A. Dorodnitsyn, "General Method of Integral Relations and its Application to Boundary Layer Theory," Advances in Aeronautical Sciences, Vol. 3 (Th. von Karman, chmn. ed. comm.), pp 207-219, Macmillan, New York, 1962.
- 4.7. O.M. Belotserkovskii, "Flow with a Detached Shock Wave about a Symmetrical Profile," J. Appl. Math. Mech. (Prikl. Mat. Mekh.), Vol. 22, pp 279-296, 1958.
- 4.8. O.M. Belotserkovskii, "The Calculation of Flow Past Axisymmetric Bodies with Detached Shock Waves (Calculation Formulae and Flow Field Tables), Vychishtel'noi Tsentr. Akad. Nauk SSSR, Moscow, 1961, Transl. as Tech. Memo. No. RAD-TM-62-64, Research and Advanced Dev. Div., Avco Corporation, Wilmington, Massachusetts, 1962; see also J. Appl. Math. Mech. (Prikl. Mat. Mekh.), Vol. 24, pp 744-755, 1960.
- 4.9. O.M. Belotserkovskii, A. Buletkaev, and V.G. Grudnitskii, "Algorithms for Numerical Schemes of the Method of Integral Relations for Calculating Mixed Gas Flows," Zh. Vychishtel'noi Mat. i Mat. Fiz., Vol. 6, pp 1064-1081, 1966; translated in U.S.S.R. Comput. Math. and Math. Phys., Vol. 1, pp 162-184, 1968.

- 4.10. O.M. Belotserkovskii, E.S. Sedova, and F.V. Shugaev, "The Supersonic Flow Round Blunt Bodies of Revolution with a Break in the Generator," Zh. Vychislitel'noi Mat. i Mat. Fiz., Volume 6, pp 930-934, 1966; translated in U.S.S.R. Comput. Math. and Math. Phys., Vol. 1, pp 210-217.
- 4.11. S.M. Gilinskii and G.F. Telenin, "The Supersonic Flow Round Bodies of Different Shapes with a Receding Shock Wave," Jzv. Akad. Navk SSSR (Series Mekh. Machinost.), No. 5, pp 148-156, 1964.
- 4.12. R. Gold, and M. Holt, "Calculation of Supersonic Flow Past a Flat-Headed Cylinder by Belotserkovskii's Method," AFOSR Tech. Note No. 59-199, Div. of Appl. Math., Brown University, Providence, R.I., 1959.
- 4.13. H.J. Deacon, Jr., and C.C. Oliver, "Application of the Method of Integral Relations to the Non-Equilibrium Hypersonic Planetary Entry Problem," Martin Company, Denver, Colorado.
- 4.14. W.C. Kuby, R.M. Foster, S.R. Byron, M. Holt, "Symmetrical, Equilibrium Flow Past a Blunt Body at Super-orbital Re-entry Speeds," AIAA Journal, Vol. 5, No. 4, pp 610-617, April 1967.
- 4.15. M. Holt, "Direct Calculation of Pressure Distribution on Blunt Hypersonic Nose Shapes with Sharp Corners," J. Aerospace Science, Vol. 28, No. 11, 1961.
- 4.16. R. Vaglio-Laurin, and A. Ferri, "Theoretical Investigation of the Flow Field about a Blunt-Nosed Body in Supersonic Flight," J. Aerospace Sci., Vol. 25, pp 761-770, 1958.
- 4.17. H. Bossel, "Inviscid and Viscous Models of the Vortex Breakdown Phenomenon," Ph.D. Thesis, University of California, Berkeley, California, August 1967.
- 4.18. PL/I Formac Interpreter, 360D, 03. 3.004, IBM.
- 4.19. H. Bossel, "A N-th Order Integral Method for Boundary Layer Flows" (Unpublished).

SECTION 5

- 5.1. O. M. Belotserkovskii, A. Buletkaev, and V. G. Grudnitskii, "Algorithms for Numerical Schemes of the Method of Integral Relations for Calculating Mixed Gas Flows", Zh. Vychishtel'noi Mat. i Mat. Fiz., 6, pp 1046-1081 (1966), translated in U.S.S.R. Comput. Math. and Math. Phys., 1, pp 162-184 (1968).
- 5.2. O.M. Belotserkovskii, "Supersonic Symmetrical Flow of Perfect and Real Gases Arond Blunt Bodies," Journal of Computing Mathematics and Mathematical Physics, Vol. II, No. 6, November-December 1962.
- 5.3. H.W. Liepmann, A. Roshko, Elements of Gasdynamics, John Wiley and Sons, Inc., New York, pp 127, 1957.

SECTION 6

- 6.1. O.M. Belotserkovskii, "The Calculation of Flow Past Axisymmetric Bodies with Detached Shock Waves (Calculation Formulae and Flow Field Tables), Vychishtel'noi Tsent. Akad. Nauk SSSR, Moscow, 1961, Transl. as Tech. Memo, No. RAD-TM-62-64, Research and Advanced Dev. Div., Avco Corporation, Wilmington, Massachusetts, 1962; see also J. Appl. Math. Mech. (Prikl. Mat. Mekh.) 24, pp 744-755, 1960.